Published in final edited form as:
J Comp Neurol. 2007 June 1; 502(4): 563–583. doi:10.1002/cne.21330.

Distribution of Tuberoinfundibular Peptide of 39 Residues and Its Receptor, Parathyroid Hormone 2 Receptor, in the Mouse Brain

CATHERINE A. FABER[1], **ARPÁD DOBOLYI**[2], **MARK SLEEMAN**[3], and **TED B. USDIN**[1,*]

[1] Section on Fundamental Neuroscience, National Institute of Mental Health, Bethesda, Maryland 20892

[2] Neuromorphological and Neuroendocrinological Research Laboratory, Hungarian Academy of Sciences and Semmelweis University, Budapest, Hungary, 1094

[3] Regeneron Pharmaceuticals Inc., Tarrytown, New York, 10591

Abstract

Tuberoinfundibular peptide of 39 residues (TIP39) was identified as a potent parathyroid hormone 2 receptor (PTH2R) agonist. Existing anatomical data also support the suggestion that TIP39 is the PTH2R's endogenous ligand, but a comprehensive comparison of TIP39 and PTH2R distributions has not been performed. In the present study, we compared the distributions of TIP39 and PTH2R on adjacent mouse brain sections. In addition, we determined the locations of PTH2R-expressing cell bodies by in situ hybridization histochemistry and by labeling β-galactosidase driven by the PTH2R promoter in knockin mice. An excellent correlation was found between the distributions of TIP39-containing fibers and PTH2R-containing cell bodies and fibers throughout the brain. TIP39 and the PTH2R are abundant in medial prefrontal, insular, and ectorhinal cortices, the lateral septal nucleus, the bed nucleus of the stria terminalis, the fundus striati, the amygdala, the ventral subiculum, the hypothalamus, midline and intralaminar thalamic nuclei, the medial geniculate body, the periaqueductal gray, the ventral tegmental area, the superior and inferior colliculi, the parabrachial nuclei, the locus coeruleus, subcoeruleus and periolivary areas, and the nucleus of the solitary tract. Furthermore, even the subregional distribution of TIP39- and PTH2R-immunoreactive fibers in these regions showed remarkable similarities, providing anatomical evidence that TIP39 may act on the PTH2R. Based on these observations and on previous pharmacological data, we propose that TIP39 is an endogenous ligand of the PTH2R and that they form a neuromodulator system, which is optimally positioned to regulate limbic, endocrine, and auditory brain functions.

Indexing terms

tuberoinfundibular peptide of 39 residues; parathyroid hormone 2 receptor; TIP39 and PTH2 receptor in situ hybridization and immunocytochemistry; neuropeptide; neuromodulator; neuroanatomical distribution; transgenic mouse; promoter driven expression

---

The parathyroid hormone 2 receptor (PTH2R) was identified on the basis of its sequence homology to other polypeptide-recognizing receptors (Usdin et al., 1995). It is a seven transmembrane domain receptor, which belongs to the type II (or family B) class of G-

*Correspondence to: Dr. Ted B. Usdin, Section on Fundamental Neuroscience, National Institute of Mental Health, 35 Convent Dr., Bethesda, MD 20892-4094. usdint@mail.nih.gov.

protein-coupled receptors (Harmar, 2001; Usdin et al., 2002). It has about 50% amino acid sequence similarity with the parathyroid hormone 1 receptor (PTH1R). Following up on pharmacological and distributional data suggesting that parathyroid hormone and parathyroid hormone-related peptide are not endogenous ligands of PTH2R, tuberoinfundibular peptide of 39 residues (TIP39) was purified from bovine hypothalamus (Usdin et al., 1999b) on the basis of its stimulation of cAMP formation in a PTH2R-expressing cell line. Mouse, rat, and human TIP39 were subsequently cloned (Dobolyi et al., 2002; John et al., 2002). Mouse and rat TIP39 sequences are identical, and share only 4 and 6 amino acid residues with parathyroid hormone-related peptide and parathyroid hormone, respectively. TIP39 is a potent agonist and binds to the PTH2R with high affinity, providing pharmacological support for the suggestion that TIP39 is the PTH2R's endogenous ligand. In contrast, TIP39 has low affinity and negligible agonism at the PTH1R (Usdin et al., 1999b; Usdin, 2000).

The expression and distribution of TIP39 has been investigated in detail in the rat (Dobolyi et al., 2003b). TIP39 neurons are restricted to two brain regions (Dobolyi et al., 2003b), the subparafascicular/posterior intralaminar thalamic area, which extends caudolaterally from the periventricular gray of the thalamus to the medial geniculate body, and the medial paralemniscal nucleus at the midbrain-pons junction. In contrast to the restricted distribution of TIP39 cell bodies, amplification immunocytochemistry demonstrated a widespread distribution of TIP39 fibers in limbic, endocrine, and auditory brain regions (Dobolyi et al., 2003a; Wang et al., 2006b). The expression and distribution of PTH2R has also been examined in the rat (Wang et al., 2000). PTH2R-expressing cell bodies were found in a variety of brain areas (Wang et al., 2000). However, some discrepancies were reported between PTH2R mRNA-expressing and PTH2R-immunoreactive (ir) cell bodies (Wang et al., 2000). Cells expressing PTH2R mRNA, but not immunoreactive cell bodies, were observed in the medial septum and some hypothalamic and brainstem areas. One possible explanation for these discrepancies is that it is generally difficult to detect PTH2R-ir in cell bodies. However, other possibilities cannot be excluded.

Related to the precise topographical localization of PTH2R is the question of spatial correspondence between TIP39 and the PTH2R. In order to act on the PTH2R, TIP39 has to reach the sites where it is located. The original mapping studies suggested some mismatches between the localization of TIP39 and the PTH2R (Wang et al., 2000; Dobolyi et al., 2003b). Mismatches between the distributions of neuropeptides and their putative receptors have been explained by the ability of peptides that have high affinity for their receptors to be effective at very low concentration, and therefore act following relatively long diffusion distances, as well as by the presence of peptide or receptor in some axonal or dendritic branches in which they do not have functional relevance (Herkenham, 1987; Leng and Ludwig, 2006). More precise comparison of TIP39 and PTH2R distributions would help to determine the extent of mismatch and guide investigation of the explanation. In a recent study of the PTH2R in the rat hypothalamus we improved on the previous conventional DAB immunolabeling of the PTH2R by using amplification immunocytochemistry (Dobolyi et al., 2006). This sensitive technique revealed previously undetected PTH2R-ir fibers (Dobolyi et al., 2006). These data suggest that amplification immunocytochemistry may also be a suitable technique to investigate the correlation of the localization of TP39 and the PTH2R in the mouse brain.

Initial functional studies implicate TIP39 in the modulation of some aspects of spinal nociceptive signaling (Dobolyi et al., 2002). Furthermore, *c-fos* activation associated with specific sexual or maternal functions in brain areas expressing TIP39 suggests that TIP39 neurons may be involved in reproductive regulation (Lin et al., 1998; Li et al., 1999; Holstege et al., 2003; Coolen et al., 2004) and the audiogenic stress response (Palkovits et

al., 2004). In addition, intracerebroventricular injection of TIP39 in rats produced effects that include the apparent modulation of an affective component of nociception (LaBuda and Usdin, 2004) and the regulation of the release of pituitary hormones (Ward et al., 2001; Sugimura et al., 2003; Usdin et al., 2003), as well as anxiolytic- and antidepressant-like effects (LaBuda et al., 2004). Nevertheless, investigation of the physiological functions of TIP39 in the central nervous system has been limited by the lack of tools to antagonize actions of endogenous TIP39. Future studies will use manipulation of TIP39 and PTH2R expression in transgenic mice. Knowledge of the distributions of TIP39 and the PTH2R in the mouse are necessary for the design and interpretation of experiments using such mice.

To expand on the current description of TIP39 and the PTH2R in the brain and to provide a foundation for future functional studies in transgenic mice, our objectives in this study were: 1) Description of the topographical localization of PTH2R-expressing cell bodies in the brain of adult male and female mice. 2) Mapping of the distribution of PTH2R-ir fibers in adult male and female mouse brain. 3) To determine the distribution of TIP39 in adult male and female mice in comparison to that of PTH2R. To address these questions we performed X-gal histochemical visualization of β-galactosidase in transgenic mice expressing β-galactosidase driven by the PTH2R promoter (PTH2R knockin mice). We also investigated the distribution of TIP39 and PTH2R-expressing cell bodies using in situ hybridization histochemistry in mouse brain serial sections. In addition, we compared adjacent sections immunolabeled for TIP39 and the PTH2R using fluorescent amplification immunocytochemistry.

MATERIALS AND METHODS

Animals

All procedures were performed according to approved National Institute of Mental Health (Bethesda, MD) animal care protocols and in accordance with the National Institutes of Health *Guide for the Care and Use of Laboratory Animals.* Experiments were performed on young adult (60–70 days old) mice (Taconic Farms, German-town, NY). All efforts were made to minimize the number of animals used and their suffering. A total of 46 mice were used for PTH2R in situ hybridization (two males and two females), X-gal histochemical staining (six PTH2R knockin males and three wildtype control males as well as six PTH2R knockin females and three wildtype control females), PTH2R immunolabeling (six males and six females), and TIP39 immunolabeling (six males and six females). Animals were anesthetized with sodium pentobarbital (80 mg/kg i.p.) and then decapitated for in situ hybridization or perfused for histochemistry and immunocytochemistry.

Knockin mice expressing β-galactosidase driven by the PTH2R promoter

The first protein coding exon of the mouse PTH2R gene was replaced by the bacterial lacZ coding sequence by homologous recombination in F1 (129Sv/Ev × c57Bl/6) hybrid mouse embryonic stem (ES) cells, as previously described (Valenzuela et al., 2003). Following identification of ES cells with appropriate recombination by the Regeneron group, the cells were expanded and introduced into c57Bl/6 blastocysts in the NIMH transgenic mouse core facility. Resulting mice were back-crossed with C57Bl/6 mice. Heterozygous animals were used for the experiments in this study. Knockin mice were identified by polymerase chain reaction (PCR)-based genotyping on DNA from tail biopsies using primers for lacZ or one primer in the inserted sequence and one primer in the flanking gene sequence.

Primer sequences were: 5′-GCGCTGGTTGATTAGATACC, P2R_HDR2-B; 5′-GCTTCCTCGTGCTTTACGGTATC, Neo_3′b; and 5′-

GAGAGGCTGTTTGTAGAAGGCTGA, P2R_64264U, which produced bands of 260 base-pairs from the wildtype allele and 700 from the knockin allele.

X-gal labeling

PTH2R knockin mice (six males and six females) as well as wild type control littermates (three males and three females) were used to visualize the β-galactosidase marker enzyme histochemically. Mice were anesthetized and perfused transcardially with 10 mL phosphate-buffered saline (PBS; pH 7.4) followed by 30 mL of cold 2% paraformaldehyde/0.2% glutaraldehyde mixture dissolved in PBS. Brains were removed, postfixed in 0.2% glutaraldehyde in PBS overnight, and coronal sections of 50 μm thickness were cut on a vibrating microtome from bregma level of 3 mm to −8 mm. Sections were washed twice for 10 minutes each in wash buffer (100 mM phosphate buffer at pH 7.4, 2 mM $MgCl_2$, 0.01% Na-deoxycholate, and 0.02% octylphenol-ethylene oxide condensate [Nonidet P-40]). Then the sections were incubated in freshly made staining solution containing 5 mM potassium ferricyanide, 5 mM potassium ferrocyanide, and 1 mg/mL X-gal (5-bromo-4-chloro-3-indolyl-D-galactopyranoside) dissolved in wash buffer at room temperature in darkness overnight. Sections were then washed twice in 50 mM Tris buffer (pH 8.0), mounted on positively charged slides, and cover-slipped with mounting medium (Cytoseal 60; Stephens Scientific, Kalamazoo, MI).

In situ hybridization histochemistry

Brains were removed and quickly frozen on dry ice. Coronal sections (12 μm) were cut using a cryostat from bregma level 3 mm to −8 mm, mounted on positively charged slides (SuperfrostPlus, Fisher Scientific, Pittsburgh, PA), dried, and stored at −80°C until use. In situ hybridization protocols are described in detail on the Web (http://intramural.nimh.nih.gov/lcmr/snge/Protocols/ISHH/ISHH.html). [^{35}S]UTP-labeled riboprobes were generated using a MAXIscript transcription kit (Ambion, Austin, TX) from PCR-amplified fragments of the TIP39 cDNA subcloned into the vector pBluescript (Stratagene, La Jolla, CA). Antisense riboprobes were prepared using T7 RNA polymerase. A region of the rat TIP39 cDNA sequence corresponding to amino acids −55 to 37, where amino acid 1 is the first residue of mature TIP39, was used to generate probes. We have shown previously in rats that this antisense probe produces equivalent hybridization patterns to probes with nonoverlapping sequences corresponding to amino acids −55 to −18, and −17 to 37 (Dobolyi et al., 2003b). Similarly, a region of the rat PTH2R cDNA sequence corresponding to bases 482–864 was used to generate probes. We have shown previously that this antisense probe produces equivalent hybridization patterns to probes with the nonoverlapping sequence corresponding to bases 1274–1828 (Wang et al., 2000). Following hybridization and washes, slides were dipped in NTB2 nuclear track emulsion (Eastman Kodak, Rochester, NY) and stored at 4°C for 3 weeks. Then the slides were developed and fixed with Kodak Dektol developer and Kodak fixer, respectively, counterstained with Giemsa, and coverslipped with mounting medium (Cytoseal 60; Stephens Scientific).

Immunocytochemistry

PTH2R antiserum—PTH2R was detected with an affinity-purified antiserum from a rabbit immunized with the synthetic peptide RQIDSHVTLPGYVWSSSEQDC, corresponding to residues 480–500 of the rat PTH2R (GenBank Entry U55836), conjugated to keyhole limpet hemocyanin. This antiserum (from rabbit #2710) has previously been used and characterized (Usdin et al., 1999a; Wang et al., 2000) as summarized below. The deduced rat and human receptor sequences differ at only 3 out of the 21 amino acids in this sequence, so we attempted to use cells expressing the cloned human receptor to examine the specificity of the antiserum. Antiserum from two rabbits immunized with this peptide

produce strong immunolabeling of HEK293 cells stably expressing the human PTH2R. Preimmune serum does not label the PTH2R-expressing cells, and no labeling of either the parent HEK293 cells or HEK293 cells stably expressing the human PTH1R is detected. Similarly, there is intense labeling of 20–30% of COS-7 cells transfected with PTH2R cDNA but no labeling of cells in mock-transfected cultures. Several bands are labeled in Western blots of PTH2R-enriched membranes, probably representing a combination of multiple glycosylation states and aggregation or oligomerization of the receptor. The highest mobility major band migrates with an apparent molecular weight of 84K, consistent with the size seen following Western blotting of a C-terminal epitope labeled PTH2R, and labeling of the receptor with a radioactive photoaffinity ligand. Following digestion with PNGase F, the mobility of the high mobility major band increases to an apparent molecular weight of 63K, consistent with the predicted size of the protein based on its cDNA sequence. No signal is seen in membranes prepared from the parent HEK293 cells or ones expressing PTH1R. Only 4 out of the 21 residues are the same as those in the human, mouse, or rat PTH1R and no significant labeling is detected in rat kidney tubules. Absorption of the antiserum with the peptide used to generate it eliminates tissue labeling and specific staining is absent when preimmune serum is used to label tissue.

TIP39 antiserum—TIP39 was detected with an affinity-purified antiserum from a rabbit immunized with mouse (m) TIP39 coupled to keyhole limpet hemocyanin by 1-ethyl-3-(3-dimethylaminopropyl)carbodiimide. This antiserum (pooled from rabbits #7250 and #7251) has previously been used and characterized (Dobolyi et al., 2002, 2003a,b) as summarized below. The titer (50% maximum binding to immobilized peptide) of the affinity-purified anti-mTIP39 antiserum against mTIP39 was 3 ng/mL. Immunolabeling with the affinity-purified anti-mTIP39 was abolished by overnight preincubation at room temperature of a working dilution of the antiserum with 1 μM synthetic mTIP39 (a sample treated identically except for omission of the peptide produced strong labeling). The anti-mTIP39 antiserum exhibited less than 1% crossreactivity with parathyroid hormone and no detectable crossreactivity with other peptides tested including parathyroid hormone-related peptide, calcitonin, substance P, vasoactive intestinal peptide, glucagon, and calcitonin gene-related peptide (Dobolyi et al., 2002). The anti-mTIP39 antiserum labels cell bodies in rat with exactly the same distribution as observed by in situ hybridization histochemistry with probes directed against TIP39 mRNA (Dobolyi et al., 2003b). In addition, TIP39 immunolabeling disappears from fibers following lesion of the distant TIP39 cell bodies (Dobolyi et al., 2003a).

Immunostaining protocol—Mice (12 males and 12 females) were anesthetized and perfused transcardially with 10 mL PBS followed by 30 mL ice-cold buffered (pH 7.4) 4% paraformaldehyde dissolved in PBS. The brains and spinal cords were removed, postfixed in buffered 4% paraformaldehyde overnight, washed for at least 3 days with PBS (pH 7.4), embedded in 2% gelatin, and then 50-μm thick sections were cut with a vibrating microtome from bregma level of 3 mm to −8 mm in mice. Free-floating sections were then pretreated with 1% bovine serum albumin in PBS containing 0.5% Triton X-100 for 30 minutes at room temperature. The sections were then placed in anti-TIP39 primary antiserum (1:3,000 for tyramide amplification and 1:600 for DAB reaction) for 48 hours at room temperature or anti-PTH2 receptor primary antiserum (1:60,000 for tyramide amplification and 1:15,000 for DAB reaction) for 24 hours at room temperature as described previously (Wang et al., 2000; Dobolyi et al., 2003b). The sections were then incubated in biotinylated antirabbit secondary antibody (1:600 dilution; Vector Laboratories, Burlingame, CA) for 2 hours followed by incubation in a solution containing avidin-biotin-peroxidase complex (1:150; Vector Laboratories) for 2 hours. The sections were then treated with 0.06% DAB or FITC-tyramide (1:20,000) and H_2O_2 in Tris hydrochloride buffer (0.1 M, pH 8.0) for 10 minutes

as described previously (Hunyady et al., 1996). Sections were then washed twice in 50 mM Tris buffer (pH 8.0) and mounted on positively charged slides. Finally, the sections were cover-slipped with antifade medium (Prolong Antifade Kit, Molecular Probes, Eugene, OR) for fluorescence, and with Cytoseal 60 mounting medium (Stephens Scientific) for DAB sections.

Histological analyses

The naming of anatomical regions is based on the "Mouse Brain in Stereotaxic Coordinates" by Franklin and Paxinos (1997). Images captured at 1300 × 1030 pixel resolution with a Zeiss Axiocam HR digital camera on an Zeiss Axioplan2 light microscope equipped with fluorescent epi-illumination using a 5× objective. Montages were assembled from individual pictures using the MosaiX function in Zeiss Axiovision software. Contrast was adjusted using the "levels" and "sharpness" commands in Adobe Photoshop CS 8.0 (San Jose, CA) and images were cropped for illustration. Full resolution was maintained until the photomicrographs were finalized, at which point images were adjusted to a resolution of 300 dpi.

RESULTS

We identified two areas in the mouse brain where neurons expressed TIP39 using both in situ hybridization histochemistry and immunocytochemistry. In contrast, we found a widespread distribution of PTH2R-expressing neurons using in situ hybridization histochemistry and X-gal labeling in PTH2R knockin mice. In addition, immunolabeling of TIP39 and the PTH2R demonstrated similar distributions of TIP39- and PTH2R-containing neuronal fibers in many brain areas.

Distribution of TIP39-expressing cell bodies

In situ hybridization histochemistry and immunocytochemistry revealed the same distribution of TIP39-expressing perikarya in male and female mice, and there was no apparent topographical difference between the genders. The posterior intralaminar complex of the thalamus is one of the two brain areas that contained TIP39 neurons. Medially, TIP39 neurons were distributed in the subparafascicular area between the midline and the fasciculus retroflexus (Fig. 1A). These cells were contiguous with more laterally and caudally located TIP39 neurons in the parvicellular subparafascicular nucleus immediately above the fibers of the medial lemniscus (Fig. 1B). Further laterally and more caudally, TIP39 neurons were located in the posterior intralaminar nucleus of the thalamus and in its surrounding area ventromedial to the medial geniculate body (Fig. 1C). The medial paralemniscal nucleus at the midbrain-pons junction is the other brain area that contained TIP39 perikarya (Fig. 1D). These TIP39 neurons were located immediately dorsal to the rubrospinal tract and medial to the fibers of the lateral lemniscus.

Distribution of PTH2R-expressing cell bodies

X-gal labeling of cells was usually confined to the nucleus and appeared as small blue dots. Occasionally, a few large neurons including some motor neurons, pyramidal cells, and Purkinje cells exhibited a light blue labeling in their perikarya. We did not consider this signal specific and did not include these very large-sized cells in our description. In situ hybridization histochemistry and the specific X-gal labeling in PTH2R knockin mice revealed the same distribution of PTH2R-expressing neurons in all but a few brain areas, where only X-gal signal was observed (see below). The distribution of labeling was the same in male and female mice with either technique.

Cerebral cortex—PTH2R-expressing neurons were distributed throughout the cerebral cortex, with a density that varied somewhat between regions. The density of PTH2R-expressing neurons was the highest in the infra-limbic cortex, where they were found in all cortical layers. Some additional frontal cortical regions including the pre-limbic, anterior cingulate, and insular cortices also exhibited a relatively higher density of PTH2R-expressing neurons. The density of PTH2R-expressing neurons decreased toward more caudal levels of the cerebral cortex, except for an accumulation of PTH2R-expressing neurons in the superficial layers of the ectorhinal cortex. In addition, a higher density of PTH2R-expressing neurons was found in layer 6b along the outer surface of the corpus callosum throughout the cerebral cortex (Fig. 2A,C).

Limbic system—There were a few PTH2R-expressing neurons in the anterior olfactory nucleus and in the olfactory tubercle. In the septum, only the lateral nucleus contained PTH2R-expressing neurons. This region contained a very high density of PTH2R-expressing neurons, especially in its ventral part (Fig. 2D). More rostrally, the intermediate part of the lateral septal nucleus was also rich in PTH2R neurons. Most parts of the bed nucleus of the stria terminalis contained a moderate density of PTH2R-expressing neurons. In contrast, the posteromedial part of the medial subdivision of the bed nucleus of the stria terminalis contained a very high density of PTH2R-expressing neurons (Fig. 3B). Many PTH2R-expressing neurons were present in the amygdala (Fig. 4C). The density of PTH2R-expressing neurons was high in the medial nucleus, especially in its posterodorsal subdivision. A moderate density of neurons was found in the anterior amygdaloid area, the central and cortical amygdaloid nuclei, and the amygdala-hippocampal transitional zone. A low density of scattered PTH2R-expressing neurons was present throughout the hippocampus, with a slightly higher density of PTH2R-expressing neurons in the dentate gyrus and the subiculum.

In the basal ganglia, the claustrum and the dorsal endopiriform nucleus contained a fairly large number of PTH2R-expressing neurons (Fig. 4A,C), while there was a moderate density of randomly distributed PTH2R-expressing neurons throughout the accumbens nucleus, the caudate putamen (Fig. 2A,C), the ventral striatum, and the substantia innominata.

The thalamus was relatively poor in PTH2R-expressing neurons except for a few regions. The medial subdivision of the metathalamic medial geniculate body contained a very high density of PTH2R-expressing neurons, whereas its ventral subdivision contained a moderate density of PTH2R-expressing neurons. A high to moderate density of PTH2R-expressing neurons was detected in some midline and intralaminar thalamic nuclei including the paraventricular, centrolateral, paracentral, centromedian (Fig. 4D), and reuniens (Fig. 3C) thalamic nuclei. In addition, a moderate density of PTH2R-expressing neurons was present in the epithalamic lateral habenular nucleus and the subthalamic zona incerta. Finally, X-gal labeling was present in the dorsal part of the lateral geniculate nucleus of PTH2R knockin mice, but in situ hybridization for the PTH2R did not indicate PTH2R-expressing neurons in this brain area.

PTH2R-expressing neurons were abundant in many regions of the hypothalamus. In the preoptic region, a high density of PTH2R-expressing neurons was present in the medial preoptic nucleus, whereas a low density of PTH2R-expressing neurons was seen in other parts of the medial preoptic area (Fig. 3A,B). In the anterior hypothalamic region a moderate density of PTH2R-expressing neurons was present in the paraventricular and periventricular nuclei, whereas the anterior hypothalamic nucleus contained a low density of PTH2R-expressing neurons (Fig. 3C). In the middle portion of the hypothalamus a high density of PTH2R-expressing neurons was present in the arcuate nucleus, whereas a moderate density was observed in the dorsomedial and perifornical hypothalamic nuclei, and some parts of the

lateral hypothalamic area including the so-called far-lateral hypothalamus (Forel's field) immediately next to the internal capsule (Fig. 3D). In the posterior hypothalamus a high density of PTH2R-expressing neurons was present in the medial subdivision of the superior mamillary nucleus (Fig. 5A,C), while its lateral subdivision (Fig. 5A,C), and the ventral premamillary, and the tuberomamillary nuclei contained a moderate density of PTH2R-expressing neurons. In contrast, the medial and lateral nuclei of the mamillary body did not contain PTH2R-expressing neurons.

There were relatively few PTH2R-expressing neurons in the lower brainstem and cerebellum. The midbrain contained a moderate density of PTH2R-expressing neurons in the lateral interpeduncular and paranigral nuclei and in the medial raphe nucleus, and there were a few scattered PTH2R-expressing neurons in the superior and inferior colliculi. In the pons there was a moderate to high density of PTH2R-expressing neurons in the sphenoid nucleus of the tegmental area (Fig. 6C), and in the nucleus of the trapezoid body (Fig. 6D). In addition, X-gal labeling was also present in the ventral cochlear nuclei (Fig. 6E). In the medulla the nucleus of the solitary tract contained a moderate density of PTH2R-expressing neurons and the spinal trigeminal nucleus contained a low density of PTH2R-expressing neurons. A few scattered PTH2R-expressing neurons were present in the cerebellar cortex, with a somewhat higher density in the superficial portion of the molecular layer.

TIP39- and PTH2R-containing neuronal networks and fibers

We observed the same distribution of TIP39-containing fibers in male and female mouse brains. Similarly, no difference was found in the distribution of PTH2R-containing fibers between males and females. Most strikingly, the distribution of TIP39-containing fibers was very similar to the distribution of PTH2R-containing fibers. In some brain regions, however, PTH2R-containing but not TIP39-containing fibers were observed.

The cerebral cortex, except for the medial prefrontal (Fig. 7A,B), the insular (Fig. 7C,D), and ectorhinal cortices, was largely devoid of TIP39- and PTH2R-containing fibers. In the medial prefrontal cortex the fibers were largely confined to the deep layers except within the infralimbic cortex, where fibers were also observed in the superficial layers (Fig. 7A,B). In contrast, in the insular (Fig. 7C,D) and ectorhinal cortices fibers were more abundant in the superficial layers. In addition, a few fine PTH2R-ir fibers were located along the outer surface of the corpus callosum, especially in the frontal cortices (Fig. 7B).

In the basal ganglia the core portion of the accumbens nucleus contained a moderate density of PTH2R-ir fibers and fewer TIP39-ir fibers (Figs. 7A,B, 8). In contrast, the shell portion of the accumbens nucleus contained a moderate density of both TIP39-ir and PTH2R-ir fibers (Fig. 7A,B). In the bed nucleus of the stria terminalis the lateral subdivision contained a low, while the medial subdivision a moderate to high density of TIP39-ir and PTH2R-ir fibers. In particular, a very high density of both TIP39-ir and PTH2R-ir fibers was observed in the posteromedial part of the medial subdivision of the bed nucleus of the stria terminalis (Fig. 9). The major part of the caudate-putamen was free of TIP39-ir and PTH2R-ir fibers (Fig. 8) except for a fiber bundle descending in its caudal and medial part from the stria terminalis, and its most caudal and ventral part, the fundus striati, which contained a moderately dense network of immunoreactive fibers (Fig. 11). The claustrum, the dorsal endopiriform nucleus, the ventral striatum, and the substantia innominata, including an area which overlays the nucleus basalis of Meynert, contained a low density of TIP39-ir and PTH2R-ir fibers.

Limbic system—There were a few TIP39-ir and PTH2R-ir fibers in the anterior olfactory nucleus and in the olfactory tubercle but not in the olfactory bulb. In the septum only the lateral nucleus contained TIP39-ir and PTH2R-ir fibers, but this region had a very high density of TIP39-containing fibers, especially in its intermediate and ventral parts (Fig. 8).

In this region some cells were surrounded with varicose fibers, and observation of immunostained sections at high magnification was necessary to determine that the cell bodies did not contain TIP39. Many TIP39-ir and PTH2R-ir fibers were present in the amygdala. The highest density of fibers was in the posterodorsal subdivision of the medial amygdaloid nucleus. The central nucleus (Fig. 11) and the amygdala-hippocampal transitional zone (Fig. 12) contained a moderate density of TIP39-ir and PTH2R-ir fibers, although in the former the density of PTH2R-ir fibers was less than that of TIP39-ir fibers. There was a low density of fibers in the anterior amygdaloid area, the anterior subdivision of the medial amygdaloid nucleus, and in the basomedial and cortical amygdaloid nuclei (Fig. 11), whereas the lateral and basolateral amygdaloid nuclei contained no TIP39-ir or PTH2R-ir fibers. Within the hippocampus only the ventral subiculum contained TIP39-ir and PTH2R-ir fibers (Fig. 12).

The thalamus was relatively poor in TIP39-ir and PTH2R-ir fibers except for a few regions. There was a high to moderate density of TIP39-ir fibers in the paraventricular and reuniens (Fig. 11A) thalamic nuclei. These two nuclei also contained a high density of PTH2R-ir fibers (Fig. 11B), while other midline and intralaminar thalamic nuclei including the centrolateral, paracentral, and centromedian thalamic nuclei had a low density of PTH2R-ir fibers (Fig. 11B). Additional TIP39-ir and PTH2R-ir fibers were present in the lateral posterior and ethmoid thalamic nuclei and the lateral habenular nucleus. Apart from these regions, TIP39-ir and PTH2R-ir fibers were also present in the vicinity of the TIP39-containing cell bodies in the subparafascicular area as well as in the area medial to the medial geniculate body (Fig. 12). From the latter region, TIP39-ir and PTH2R-ir fibers ran in the zona incerta between the subthalamic nucleus and the medial lemniscus to the hypothalamus as far medial as the paraventricular nucleus (Fig. 11). In addition, a moderate density of PTH2R-ir but not TIP39-ir fibers was found in the ventral part of the lateral geniculate nucleus.

TIP39-ir and PTH2R-ir fibers were abundant in many regions of the hypothalamus. In the preoptic region TIP39-ir and PTH2R-ir fibers had a high density in the medial preoptic nucleus and a low density in other parts of the medial preoptic area and the lateral preoptic area (Fig. 9). In the anterior hypothalamus a high density of TIP39-ir and PTH2R-ir fibers was present in the parvicellular subdivisions of the paraventricular nucleus and in the periparaventricular zone (Fig. 10). The latter was particularly conspicuous on the side of the magnocellular subdivisions of the paraventricular nucleus, which lack of TIP39-ir and PTH2R-ir fibers (Fig. 10). A moderate density of TIP39-ir and PTH2R-ir fibers were present in the periventricular nucleus and the anterior hypothalamic nucleus, whereas only a few immunoreactive fibers were seen in the lateral hypothalamic area and the supraoptic nucleus, and no immunoreactive fibers were present in the suprachiasmatic nucleus (Fig. 10). In the middle part of the hypothalamus, the ventrolateral subdivision of the ventromedial nucleus, and the dorsomedial and arcuate nuclei contained a high density of TIP39-ir and PTH2R-ir fibers (Fig. 11). A moderate density of TIP39-ir and PTH2R-ir fibers was present in the perifornical nucleus and some parts of the lateral hypothalamic area including the so-called far-lateral hypothalamus (Forel's fields) immediately next to the internal capsule (Fig. 11), but the immunolabeled fibers were sparse in most parts of the lateral hypothalamic area. In addition, a very dense accumulation of TIP39-containing fibers was seen along both the dorsal and ventral surfaces of the internal capsule. Some of the fibers from the dorsal bundle seemed to penetrate into the internal capsule. The ventral bundle, which may correspond to the supraoptic decussations, is located between the internal capsule and the optic tract (Fig. 11). Medially, fibers enter the lateral hypothalamus and cross over at the caudal edge of the optic chiasm (Fig. 11). In addition to the overwhelming similarities between the distributions of the TIP39-ir and PTH2R-ir fibers and fiber terminals in this region of the hypothalamus, there were also some differences. A high

density of PTH2R-ir fibers but only a few TIP39-ir fibers were present in the median eminence. In addition, there were no TIP39-ir fibers in the dorsomedial and central subdivisions of the ventromedial nucleus of the hypothalamus, whereas a low density of PTH2R-ir fibers was visible here. In the posterior hypothalamus the highest density of TIP39-ir and PTH2R-ir fibers was observed in the ventral premamillary, arcuate, and the tuberomamillary nuclei. In addition, TIP39-ir and PTH2R-ir fibers were also abundant in the posterior hypothalamic nucleus, the dorsal premamillary, supramamillary, and lateral mamillary nuclei. In contrast, the medial mamillary nuclei contained no labeled fibers.

In the midbrain a high density PTH2R-ir fibers and a somewhat lower density of TIP39-ir fibers were present in the periaqueductal gray, especially its lateral and dorsal subdivisions, and the ventral tegmental area, while the deep layers of the superior colliculus contained a moderate density of PTH2R-ir fibers and a low density of TIP39-ir fibers (Fig. 12). In addition, there was a very dense accumulation of PTH2R-ir fibers but no TIP39-ir fibers in the dorsal subdivision of the interpeduncular nucleus (Fig. 12). In contrast, a high density of both TIP39-ir and PTH2R-ir fibers was present in the deep mesencephalic nucleus (Fig. 12), the subbrachial nucleus, the intercollicular nucleus, and the external and dorsal cortices of the inferior colliculus, while the immunoreactive fibers were scarce in the central nucleus of the inferior colliculus. Fine immunoreactive fibers cross over in the commissures of the superior and inferior colliculi. TIP39-ir and PTH2R-ir fibers were also found at high density in areas near the regions of the TIP39-containing cell bodies in the medial paralemniscal nucleus. Some immunoreactive fibers could also be seen in the pretectal area, the anterior pretectal nucleus, the retrorubral field, the dorsal and median raphe nuclei, the cuneiform nucleus, and the dorsal nucleus of the lateral lemniscus. In the substantia nigra only the pars lateralis contained immunoreactive fibers. The red nucleus and the superficial layers of the superior colliculus were also largely devoid of immunoreactive fibers.

In the pons PTH2R-ir fibers were abundant in the pedunculopontine tegmental nucleus, the parabrachial nuclei, the locus coeruleus and Barrington nucleus, the subcoeruleus area, the nucleus of the trapezoid body, the dorsal periolivary nucleus, the A5 noradrenergic cell group, and the raphe magnus nucleus (Fig. 13). While the distribution of TIP39-ir fibers was very similar in these regions, their density was considerably less in some of these regions, including the parabrachial nuclei, the nucleus of the trapezoid body, and the A5 noradrenergic cell group (Fig. 13). A lower density of TIP39-ir and PTH2R-ir fibers was also observed in the supragenual nucleus, the Kölliker-Fuse nucleus, and the superior olive. Fine TIP39-ir and PTH2R-ir fibers could be seen to cross the midline at the ventral edge of the tegmentum.

There was no labeling for TIP39 and only a few scattered PTH2R-ir fibers were seen in the cerebellum. In the medulla a high density of PTH2R-ir fibers was present in the marginal layer of the spinal trigeminal nucleus and in the nucleus of the solitary tract. In contrast, there were only a few TIP39-ir fibers in the spinal trigeminal nucleus while the density of TIP39-ir fibers in the nucleus of the solitary tract was low to moderate. Other medullary regions that contained a low to moderate density of both TIP39-ir and PTH2R-ir fibers include the vestibular nuclei, the paragigantocellular nucleus, the lateral and intermediate reticular nuclei, the dorsal medullary reticular nucleus, and the cuneate nucleus.

A summary of the distribution of TIP39 and the PTH2R is shown schematically in Figure 14. As demonstrated by the schematic panels the topographical distribution of TIP39-ir fibers was, in general, very similar to that of the PTH2R-ir fibers. In addition, many brain regions that contained PTH2R-ir fibers also contained PTH2R-expressing neurons that had a very similar distribution.

DISCUSSION

We first compare the distributions of TIP39-ir and PTH2R-containing cell bodies and fibers obtained using different methods. Then we discuss evidence for the existence of a TIP39-PTH2R neuromodulator system. Finally, we propose potential functions of the TIP39-PTH2R neuromodulator system based on its location in the mouse brain.

Methodological considerations

In situ hybridization histochemistry directly visualizes the presence of RNA that is complementary to the sequence of the probe, while X-gal labeling indicates the presence of β-galactosidase activity, which appears in our knockin mice in cells in which the PTH2R promoter is active. The two different methods provided the same distribution of PTH2R-expressing cells in almost all regions, throughout many parts of the brain, which confirms their specificity. However, there were two brain regions, the dorsal part of the lateral geniculate nucleus in the thalamus and the ventral cochlear nuclei, which exhibited a strong X-gal signal without apparent in situ hybridization signal. No X-gal signal was observed in these regions in control material, so we suggest that it results either from ectopic expression of the transgene, because of insertion of foreign sequences, or mismatch between the sensitivities of the two techniques. Since PTH2R-ir fibers were not detected in these regions, we believe that the former is a more likely explanation.

The distribution of PTH2R-ir cell bodies previously described in rat (Wang et al., 2000) is, in general, similar to the distribution of PTH2R-expressing cells we report for mouse in this study. However, in this study we observed that the immunolabeling of cell bodies in mice is not reliable. Using the same staining protocol as in rats, we found many fewer and much more lightly labeled cell bodies, if any at all, in most brain regions in mice. The immunolabeling of cell bodies did not improve using an amplification immunocytochemistry staining protocol. We believe that the transport of PTH2R protein out of cell bodies and into neuronal fibers may be faster in mice than in rats. Therefore, we did not use immunocytochemistry for the description of the distribution of PTH2R-expressing cell bodies. In contrast, the immunolabeling of TIP39-containing cell bodies was satisfactory as demonstrated by the same distribution of the TIP39 in situ hybridization signal and the TIP39-ir cell bodies.

The distribution of nerve fibers and terminals was described based on an FITC-tyramine amplification immunostaining protocol. Using this protocol the labeling was comparable to the labeling of fibers in rats using the same technique. However, in rats the distribution of PTH2R-ir fibers has not been described previously using amplification immunocytochemistry except for the hypothalamus (Dobolyi et al., 2006). Since the labeling of fibers by FITC-tyramine amplification immunostaining is more intense than by the traditional DAB technique, we were able to analyze PTH2R-ir fibers throughout the brain in much more detail than in previous studies (Wang et al., 2000).

Comparison of the distributions of TIP39 and the PTH2R between mice and rats

The distribution of TIP39-expressing cell bodies determined in this study in mice was the same as that previously reported in rats (Dobolyi et al., 2003b). The distribution of TIP39-ir fibers in mice was almost the same as that in rats. Only two notable differences were detected by labeling for TIP39 and scanning a comprehensive set of mouse and rat brain sections. The density of TIP39-ir fibers was high in the medial preoptic nucleus and the ventrolateral subdivision of the ventromedial hypothalamic nucleus in mice while only moderate in rats.

The distribution of PTH2R-expressing cell bodies in mice was similar to that previously reported in rats (Wang et al., 2000) in most brain regions, including the cerebral cortex, the caudate putamen, the claustrum and endopiriform nucleus, the lateral septum, the hippocampus, the amygdala, and many thalamic, hypothalamic, and brainstem regions, and the cerebellum. There were, however, brain regions where marked differences were found in the density of PTH2R-expressing neurons between mice and rats. Most particularly, a strong in situ hybridization signal but no more than a few immunoreactive cell bodies were found in the medial septal, the ventromedial hypothalamic, the parabrachial, and the spinal trigeminal nuclei in rats (Wang et al., 2000). None of these regions contained a significant number of PTH2R-expressing cells in mice. In addition, both in situ hybridization histochemistry and immunocytochemistry revealed a high density of PTH2R-expressing neurons in the periventricular hypothalamic nucleus in rat, while this area contained only a moderate number of PTH2R-expressing neurons in mice. In contrast, there are brain regions that were abundant in PTH2R-expressing neurons in mice but do not contain a large number of PTH2R-expressing neurons in rat, including the posteromedial part of the medial division of the bed nucleus of the stria terminalis, the medial geniculate body, and the nucleus of the trapezoid body.

The distribution of PTH2R-ir fibers is also very similar between mice and rats in most brain regions including the septum, many basal ganglia nuclei, the hippocampus, the amygdala, the midline thalamic nuclei, and many hypothalamic and brainstem areas. The few notable differences when comparing our current data in mice to previously published data in rats (Wang et al., 2000) were a high to moderate density of PTH2R-ir fibers in the infralimbic and ectorhinal cortices, the ventral subiculum, the posteromedial part of the medial subdivision of the bed nucleus of the stria terminalis, the fundus striati, the zona incerta, the posterior intralaminar thalamic nuclei, the periaqueductal gray, and ventral tegmental area, and the medial parabrachial nuclei in mice and a lower density of PTH2R-ir fibers in these brain regions of rats (Wang et al., 2000). In turn, there are brain regions, where PTH2R-ir fibers were reported in rat but were not observed in mice, including the suprachiasmatic nucleus, the pars compacta and pars reticularis of the substantia nigra, the superficial layers of the superior colliculus, and the inferior olive (Wang et al., 2000). We believe that some of these differences derive from the immunostaining method used and do not represent real species differences. As discussed above, amplification immunocytochemistry and not traditional DAB immunolabeling was used in the present study.

Comparison of the distribution of TIP39 to that of the PTH2R provides anatomical evidence for a TIP39-PTH2R neuromodulator system

The localization of cell bodies that express TIP39 and those that express the PTH2R are profoundly different. TIP39 expression is confined to the subparafascicular area-posterior intralamine thalmic complex and the medial paraleminiscal nucleus, while the PTH2R is expressed in many brain regions. In contrast to the profoundly different localization of TIP39-ir and PTH2R-expressing cell bodies, the distributions of TIP39-ir and PTH2R-ir fibers are markedly similar. TIP39-ir and PTH2R-ir fibers are present in the same nuclei and areas throughout the brain except for a few areas where PTH2R-ir but not TIP39-ir fibers are abundant including the median eminence, the interpeduncular, and the spinal trigeminal nuclei. Furthermore, not only are TIP39-ir and PTH2R-ir fibers present in the same brain regions but their subregional distributions also show remarkable similarities. In fact, the two distributions are indistinguishable in most brain nuclei and areas. This finding suggests that TIP39 is available to act on the PTH2R in these brain regions and furthermore that it may act in a fairly traditional manner, with its actions focused on adjacent fibers. Together with the strong in vitro pharmacological evidence that TIP39 is a potent and high-affinity ligand for PTH2R, our anatomical data suggest that TIP39 is the endogenous ligand of the PTH2R.

Furthermore, we propose that TIP39 and the PTH2R form a neuromodulator system in many brain regions. TIP39-ir fibers are distant axons of the TIP39-expressing perikarya in the subparafascicular-ir posterior intralaminar complex and in the medial paralemniscal nuclei, which disappear following the destruction of their cell bodies (Dobolyi et al., 2003a). PTH2R-ir fibers, however, are often localized in the vicinity of PTH2R-expressing neurons. Therefore, they may represent either axons or dendrites on which TIP39 could act via the PTH2R. The finding that in a few areas PTH2R's but not TIP39 were present could be explained by the appearance of TIP39 in these areas under specific physiological conditions, although a nonfunctional expression of the PTH2R, or the existence of another ligand for the PTH2R in these areas cannot be excluded. It is possible that circulating TIP39 acts on PTH2R's in the median eminence, but a source of such TIP39 has not been observed.

Functional implications of the distribution of the TIP39-PTH2R neuromodulator system

On the basis of neuroanatomical and pharmacological observations, we proposed above that TIP39 and PTH2R constitute a TIP39-PTH2R neuromodulator system in the central nervous system. The distribution of the TIP39-PTH2R neuromodulator system suggests its involvement in limbic functions. Many of these functions involve several brain centers. Here we mention some functions in which the role of the TIP39-PTH2R neuromodulator system is supported by its localization in several of the involved brain centers and/or by initial functional studies.

The role of the TIP39-PTH2R neuromodulator system in male sexual behaviors is supported by its presence in several areas that are activated in males following mating (Sachs and Meisel, 1988; Coolen et al., 1997; Veening and Coolen, 1998; Holstege et al., 2003) including the medial preoptic nucleus, the posteromedial part of the medial subdivision of the bed nucleus of the stria terminalis, the subparafascicular area, and the posterodorsal subdivision of the medial amygdaloid nuclei. Indeed, TIP39 neurons in the subparafascicular area have been recently shown to exhibit *c-fos* activation following male sexual behavior in rats (Wang et al., 2006a). Additional brain regions have also been suggested to be parts of an interconnected network of reproductive brain centers and play a role in female sexual behaviors, lactation, and female maternal behaviors including the medial prefrontal cortex, the lateral septum, the medial preoptic, periventricular hypothalamic, arcuate and premamillary nuclei, the amygdalo-hippocampal transitional zone, the ventral tegmental area, and the periaqueductal gray (Gorski, 1985; Sachs and Meisel, 1988; Lonstein and Stern, 1997; Numan and Sheehan, 1997; Pfaus and Heeb, 1997; Li et al., 1998, [1999]; Veening and Coolen, 1998; Simerly, 2002; Holstege et al., 2003; Numan and Insel, 2003; Hasen and Gammie, 2005). The TIP39-PTH2R neuromodulator system is abundant in these brain regions, suggesting a role in reproductive behaviors.

Another potential function of the TIP39-PTH2R neuromodulator system is involvement in the processing of nociceptive and vegetative sensory input to the limbic system, which is suggested by its presence in brain areas that may participate in such information processing (Benarroch, 2006) including the nucleus of the solitary tract, the parabrachial nuclei, the midline thalamic nuclei, the paraventricular hypothalamic nucleus, the insular and infralimbic cortices. This suggestion is also supported by our previous finding that intracerebroventricular injection of TIP39 decreases pain-related affective behavior (LaBuda and Usdin, 2004).

Possibly related to limbic functions of the TIP39-PTH2R neuromodulator system is its optimal position to influence the hypothalamo-pituitary axis through its presence in the preoptic area, the arcuate, periventricular and paraventricular hypothalamic nuclei. Indeed, in vitro evidence suggests that TIP39 may influence the release of luteinizing hormone,

growth hormone, and adrenocorticotropin from the pituitary (Ward et al., 2001; Usdin et al., 2003).

The TIP39-PTH2R neuromodulator system may also be involved in the processing of auditory information because it is present in several auditory brain centers including the ectorhinal cortex, the medial geniculate body and surrounding auditory thalamic areas, the deep layers of the superior colliculus, the external cortex of the inferior colliculus, the nucleus of the trapezoid body, and possibly the ventral cochlear nuclei. In the higher auditory centers the TIP39-PTH2R neuromodulator system is typically located in nontonotopically organized regions. Therefore, we propose that the TIP39-PTH2R neuromodulator system may modulate auditory processes that do not require tonotopic information such as acoustic fear-conditioning or the loud noise-induced stress response. Such potential functions of the TIP39-PTH2R neuromodulator system are supported by the loud noise-induced *c-fos* activation in posterior intralaminar and medial paralemniscal TIP39 neurons (Palkovits et al., 2004).

In conclusion, the present article first described the precise distribution of PTH2R-expressing cell bodies by using knockin mice expressing β-galactosidase driven by the PTH2R promoter and comparing the location of β-galactosidase-positive cells to the location of PTH2R mRNA-containing cells visualized by in situ hybridization histochemistry. In addition, a very good correlation was found between the distributions of TIP39-containing fibers and PTH2R-containing cell bodies and fibers throughout the brain. Furthermore, even the subregional distribution of TIP39-ir and PTH2R-ir fibers showed remarkable similarities, providing anatomical evidence that TIP39 may act on the PTH2R. Based on this finding and on previous pharmacological evidence, we propose that TIP39 is an endogenous ligand of the PTH2R and that they form a neuromodulator system, which is optimally positioned to regulate limbic, endocrine, and auditory brain functions.

Acknowledgments

We thank Andrew Murphy, David Valenzuela, and George Yancopolos for help with the generation of the targeted ES cells, Miklós Palkovits for critically reading the article, Charles R. Gerfen for initial instructions in the scanning procedure, Timothy Reardon for technical support, and Jim Pickel and the NIMH transgenic core facility for establishing the PTH2R knockin line.

Grant sponsor: National Institute of Mental Health Intramural Research Program.

Abbreviations

A5	A5 noradrenergic cell group
ac	Anterior commissure
Acc	Accumbens nucleus
AH	Anterior hypothalamic nucleus
AHi	Amygdalo-hippocampal transitional area
Arc	Arcuate nucleus
BST	Bed nucleus of the stria terminalis
BSTMPM	BST, medial subdivision, posteromedial part
cc	Corpus callosum
Ce	Cerebellum

CeA	Central amygdaloid nucleus
CoA	Cortical amygdaloid nucleus
CL	Centrolateral thalamic nucleus
Cl	Claustrum
CM	Centromedian thalamic nucleus
CP	Caudate putamen
Cx	Cerebral cortex
DEn	Dorsal endopiriform nucleus
DM	Dorsomedial hypothalamic nucleus
DP	Dorsal peduncular cortex
DpMe	Deep mesencephalic nucleus
DR	Dorsal raphe nucleus
Ect	Ectorhinal cortex
f	Fornix
fr	Fasciculus retroflexus
FS	Fundus striati
H	Hippocampus
ic	Internal capsule
IL	Infralimbic cortex
Ins	Insular cortex
IP	Interpeduncular nucleus
LC	Locus coeruleus
LDTg	Laterodorsal tegmental nucleus
LH	Lateral hypothalamic area
ll	Lateral lemniscus
LPO	Lateral preoptic area
LS	Lateral septal nucleus
LSi	Lateral septal nucleus, intermediate subdivision
LSv	Lateral septal nucleus, ventral subdivision
LV	Lateral ventricle
m	Midline
MeA	Medial amygdaloid nucleus
MG	Medial geniculate body
MGD	Medial geniculate nucleus, dorsal subdivision
MGM	Medial geniculate nucleus, medial subdivision
MGV	Medial geniculate nucleus, ventral subdivision

ml	Medial lemniscus
MPN	Medial preoptic nucleus
MRe	Intramamillary recess of the third ventricle
MS	Medial septum
mSPF	Medial subparafascicular area
mt	Mamillothalamic tract
ot	Optic tract
PAG	Periaqueductal gray
PB	Parabrachial nuclei
PC	Paracentral thalamic nucleus
pc	Posterior commissure
Pe	Periventricular hypothalamic nucleus
Pir	Piriform cortex
PIL	Posterior intralaminar nucleus of the thalamus
POA	Periolivary area
PTH2R	Parathyroid hormone 2 receptor
PVN	Paraventricular hypothalamic nucleus
PVT	Paraventricular thalamic nucleus
py	Pyramidal tract
Re	Reuniens thalamic nucleus
RMg	Raphe magnus nucleus
rs	Rubrospinal tract
S	Subiculum
SC	Superior colliculus
SCh	Suprachiasmatic nucleus
scp	Superior cerebellar peduncle
sm	Stria medullaris
SPF	Subparafascicular area
SPFp	Parvicellular subparafascicular nucleus
Sph	Sphenoid nucleus
SubC	Subcoeruleus area
SuMM	Supramamillary nucleus, medial subdivision
TIP39	Tuberoinfundibular peptide of 39 residues
Tz	Nucleus of the trapezoid body
VMH	Ventromedial hypothalamic nucleus
VTA	Ventral tegmental area

ZI	Zona incerta
3V	Third ventricle
4V	Fourth ventricle
7n	Root of the facial nerve

LITERATURE CITED

Benarroch EE. Pain-autonomic interactions. Neurol Sci 2006;27(Suppl 2):S130–133. [PubMed: 16688616]

Coolen LM, Peters HJ, Veening JG. Distribution of fos immunoreactivity following mating versus anogenital investigation in the male rat brain. Neuroscience 1997;77:1151–1161. [PubMed: 9130794]

Coolen LM, Allard J, Truitt WA, McKenna KE. Central regulation of ejaculation. Physiol Behav 2004;83:203–215. [PubMed: 15488540]

Dobolyi A, Ueda H, Uchida H, Palkovits M, Usdin TB. Anatomical and physiological evidence for involvement of tuberoinfundibular peptide of 39 residues in nociception. Proc Natl Acad Sci U S A 2002;99:1651–1656. [PubMed: 11818570]

Dobolyi A, Palkovits M, Bodnar I, Usdin TB. Neurons containing tuberoinfundibular peptide of 39 residues project to limbic, endocrine, auditory and spinal areas in rat. Neuroscience 2003a; 122:1093–1105. [PubMed: 14643775]

Dobolyi A, Palkovits M, Usdin TB. Expression and distribution of tuberoinfundibular peptide of 39 residues in the rat central nervous system. J Comp Neurol 2003b;455:547–566. [PubMed: 12508326]

Dobolyi A, Irwin S, Wang J, Usdin TB. The distribution and neurochemistry of the parathyroid hormone 2 receptor in the rat hypothalamus. Neurochem Res 2006;31:227–236. [PubMed: 16570212]

Franklin, KBJ.; Paxinos, G. The mouse brain in stereotaxic coordinates. San Diego: Academic Press; 1997.

Gorski RA. Sexual dimorphisms of the brain. J Anim Sci 1985;61(Suppl 3):38–61. [PubMed: 3908433]

Harmar AJ. Family-B G-protein-coupled receptors. Genome Biol 2001;2:3013.

Hasen NS, Gammie SC. Differential fos activation in virgin and lactating mice in response to an intruder. Physiol Behav 2005;84:681–695. [PubMed: 15885244]

Herkenham M. Mismatches between neurotransmitter and receptor localizations in brain: observations and implications. Neuroscience 1987;23:1–38. [PubMed: 2891080]

Holstege G, Georgiadis JR, Paans AM, Meiners LC, van der Graaf FH, Reinders AA. Brain activation during human male ejaculation. J Neurosci 2003;23:9185–9193. [PubMed: 14534252]

Hunyady B, Krempels K, Harta G, Mezey E. Immunohistochemical signal amplification by catalyzed reporter deposition and its application in double immunostaining. J Histochem Cytochem 1996;44:1353–1362. [PubMed: 8985127]

John MR, Arai M, Rubin DA, Jonsson KB, Juppner H. Identification and characterization of the murine and human gene encoding the tuberoinfundibular peptide of 39 residues. Endocrinology 2002;143:1047–1057. [PubMed: 11861531]

LaBuda CJ, Usdin TB. Tuberoinfundibular peptide of 39 residues decreases pain-related affective behavior. Neuroreport 2004;15:1779–1782. [PubMed: 15257146]

LaBuda CJ, Dobolyi A, Usdin TB. Tuberoinfundibular peptide of 39 residues produces anxiolytic and antidepressant actions. Neuroreport 2004;15:881–885. [PubMed: 15073536]

Leng G, Ludwig M. Jacques Benoit lecture. Information processing in the hypothalamus: peptides and analogue computation. J Neuroendocrinol 2006;18:379–392. [PubMed: 16684129]

Li C, Chen P, Smith MS. Neural populations in the rat forebrain and brainstem activated by the suckling stimulus as demonstrated by c-fos expression. Neuroscience 1999;94:117–129. [PubMed: 10613502]

Lin SH, Miyata S, Matsunaga W, Kawarabayashi T, Nakashima T, Kiyohara T. Metabolic mapping of the brain in pregnant, parturient and lactating rats using fos immunohistochemistry. Brain Res 1998;787:226–236. [PubMed: 9518626]

Lonstein JS, Stern JM. Role of the midbrain periaqueductal gray in maternal nurturance and aggression: C-fos and electrolytic lesion studies in lactating rats. J Neurosci 1997;17:3364–3378. [PubMed: 9113892]

Numan, M.; Insel, TR. The neurobiology of parental behavior. New York: Springer; 2003.

Numan M, Sheehan TP. Neuroanatomical circuitry for mammalian maternal behavior. Ann N Y Acad Sci 1997;807:101–125. [PubMed: 9071346]

Palkovits M, Dobolyi A, Helfferich F, Usdin TB. Localization and chemical characterization of the audiogenic stress pathway. Ann N Y Acad Sci 2004;1018:16–24. [PubMed: 15240348]

Pfaus JG, Heeb MM. Implications of immediate-early gene induction in the brain following sexual stimulation of female and male rodents. Brain Res Bull 1997;44:397–407. [PubMed: 9370204]

Sachs, BD.; Meisel, RL. The physiology of male sexual behavior. In: Knobil, E.; Meill, J., editors. The physiology of reproduction. New York: Raven Press; 1988.

Simerly RB. Wired for reproduction: Organization and development of sexually dimorphic circuits in the mammalian forebrain. Annu Rev Neurosci 2002;25:507–536. [PubMed: 12052919]

Sugimura Y, Murase T, Ishizaki S, Tachikawa K, Arima H, Miura Y, Usdin TB, Oiso Y. Centrally administered tuberoinfundibular peptide of 39 residues inhibits arginine vasopressin release in conscious rats. Endocrinology 2003;144:2791–2796. [PubMed: 12810532]

Usdin TB. The PTH2 receptor and TIP39: a new peptide-receptor system. Trends Pharmacol Sci 2000;21:128–130. [PubMed: 10740285]

Usdin TB, Gruber C, Bonner TI. Identification and functional expression of a receptor selectively recognizing parathyroid hormone, the PTH2 receptor. J Biol Chem 1995;270:15455–15458. [PubMed: 7797535]

Usdin TB, Hilton J, Vertesi T, Harta G, Segre G, Mezey E. Distribution of the parathyroid hormone 2 receptor in rat: immunolocalization reveals expression by several endocrine cells. Endocrinology 1999a;140:3363–3371. [PubMed: 10385434]

Usdin TB, Hoare SR, Wang T, Mezey E, Kowalak JA. TIP39: a new neuropeptide and PTH2-receptor agonist from hypothalamus. Nat Neurosci 1999b;2:941–943. [PubMed: 10526330]

Usdin TB, Bonner TI, Hoare SR. The parathyroid hormone 2 (PTH2) receptor. Receptors Channels 2002;8:211–218. [PubMed: 12529938]

Usdin TB, Dobolyi A, Ueda H, Palkovits M. Emerging functions for tuberoinfundibular peptide of 39 residues. Trends Endocrinol Metab 2003;14:14–19. [PubMed: 12475607]

Valenzuela DM, Murphy AJ, Frendewey D, Gale NW, Economides AN, Auerbach W, Poueymirou WT, Adams NC, Rojas J, Yasenchak J, Chernomorsky R, Boucher M, Elsasser AL, Esau L, Zheng J, Griffiths JA, Wang X, Su H, Xue Y, Dominguez MG, Noguera I, Torres R, Macdonald LE, Stewart AF, DeChiara TM, Yancopoulos GD. High-throughput engineering of the mouse genome coupled with high-resolution expression analysis. Nat Biotechnol 2003;21:652–659. [PubMed: 12730667]

Veening JG, Coolen LM. Neural activation following sexual behavior in the male and female rat brain. Behav Brain Res 1998;92:181–193. [PubMed: 9638960]

Wang T, Palkovits M, Rusnak M, Mezey E, Usdin TB. Distribution of parathyroid hormone-2 receptor-like immunoreactivity and messenger rna in the rat nervous system. Neuroscience 2000;100:629–649. [PubMed: 11098126]

Wang J, Coolen LM, Brown JL, Usdin TB. Neurons containing tuberoinfundibular peptide of 39 residues are activated following male sexual behavior. Neuropeptides 2006a;40:403–408. [PubMed: 17056109]

Wang J, Palkovits M, Usdin TB, Dobolyi A. Forebrain projections of tuberoinfundibular peptide of 39 residues (TIP39)-containing subparafascicular neurons. Neuroscience 2006b;138:1245–1263. [PubMed: 16458435]

Ward HL, Small CJ, Murphy KG, Kennedy AR, Ghatei MA, Bloom SR. The actions of tuberoinfundibular peptide on the hypothalamo-pituitary axes. Endocrinology 2001;142:3451–3456. AQ—AQ1: No scale bar in figure. [PubMed: 11459790]

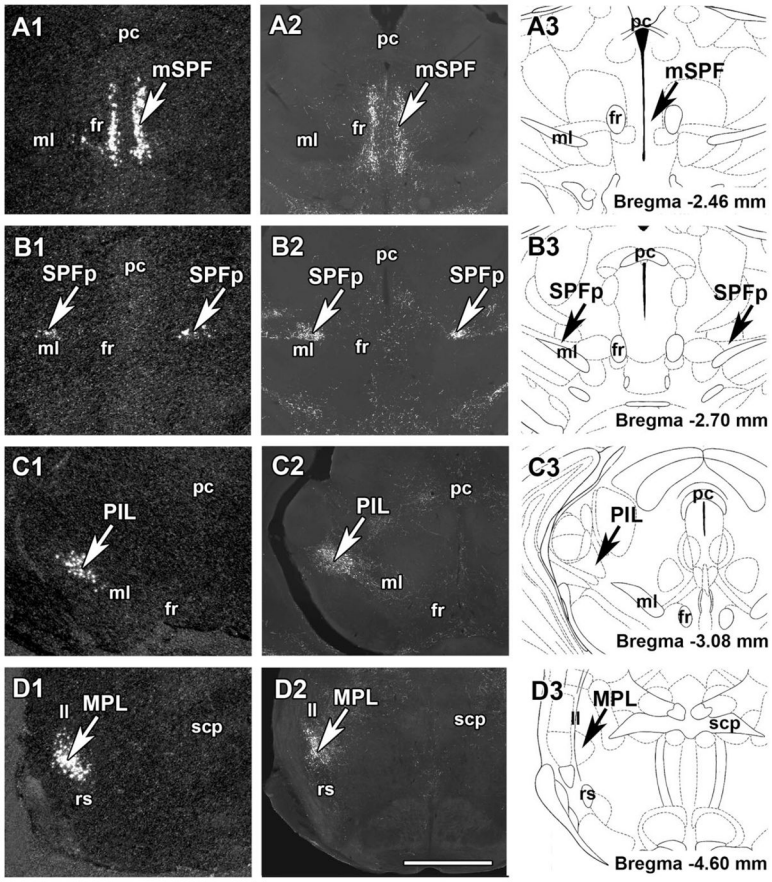

Fig. 1.

TIP39-containing neurons in the mouse brain. **A1–3:** TIP39$^+$ neurons in the medial subparafascicular area at the thalamus-midbrain junction. **B1–3:** TIP39$^+$ neurons continue into the parvicellular subparafascicular nucleus. **C1–3:** TIP39$^+$ neurons continue further laterally in the posterior intralaminar nucleus of the thalamus and surrounding areas medial to the medial geniculate body. **D1–3:** A separate group of TIP39$^+$ neurons in the medial paralemniscal nucleus at the midbrain-pons junction. A1, B1, C1, D1: TIP39 mRNA expression is demonstrated in darkfield following in situ hybridization histochemistry. A2, B2, C2, D2: TIP39 immunoreactivity is demonstrated by following fluorescent amplification immunocytochemistry. TIP39$^+$ cell bodies and TIP39$^+$ fibers are visible in the same areas. A3, B3, C3, D3: Schematic diagrams of brain regions containing TIP39$^+$ cells. Arrows point to the location of brain regions that contain TIP39$^+$ neurons. Scale bar = 1 mm.

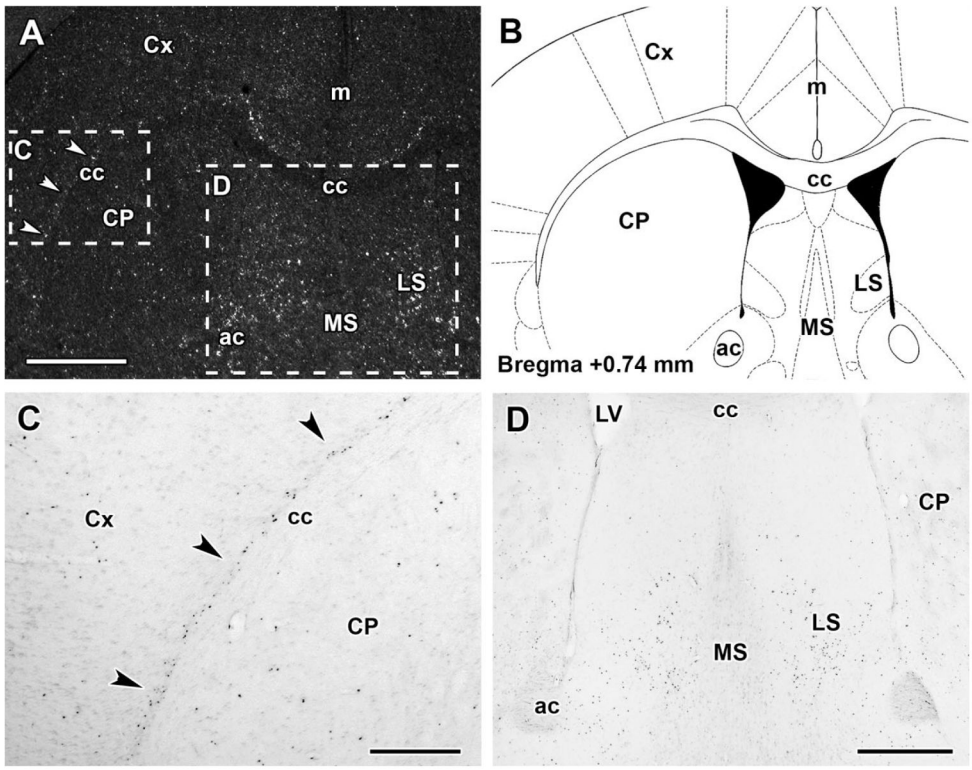

Fig. 2.

PTH2R-expressing neurons in the septal region of the mouse brain. **A:** Darkfield image of an in situ hybridization section demonstrates the location of PTH2R mRNA in the cerebral cortex, the caudate putamen, and the septum. **B:** Schematic diagram of the area corresponding to A. **C:** Scattered $PTH2R^{+}$ neurons are demonstrated by X-gal histochemistry in the cerebral cortex and the caudate putamen of a PTH2R knockin mouse. In addition, arrowheads indicate $PTH2R^{+}$ neurons lined up in the innermost layer of the cerebral cortex along the corpus callosum. The photomicrograph corresponds to the area framed in A. **D:** X-gal histochemistry in the septal region of a PTH2R knockin mouse. The photomicrograph corresponds to the area framed in A. $PTH2R^{+}$ neurons are abundant in the ventral subdivision as well as in the ventral part of the intermediate subdivision of the lateral septal nucleus. Scale bars = 1 mm in A; 300 μm in C; 500 μm in D.

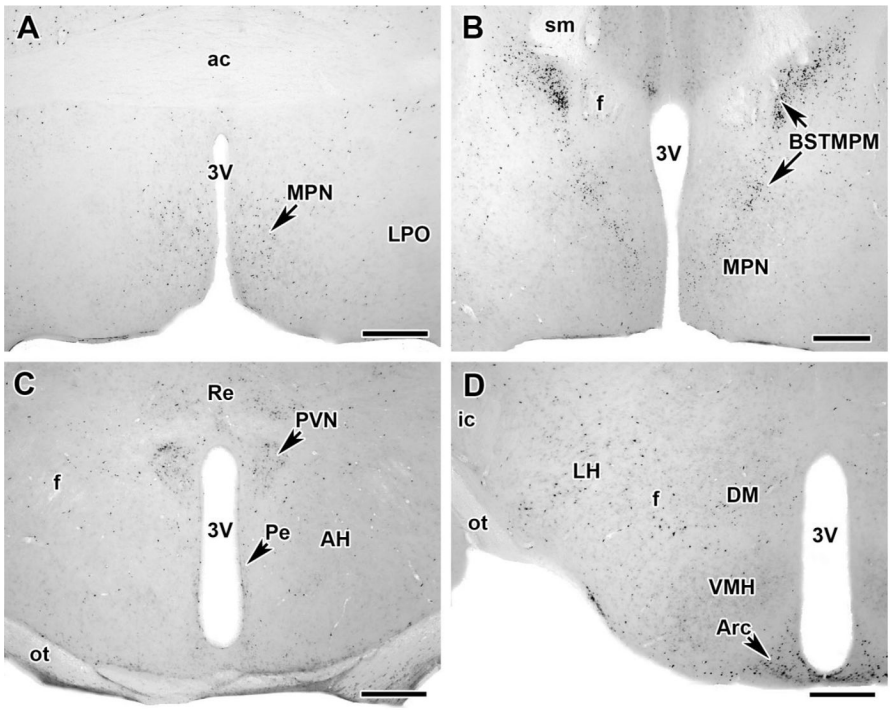

Fig. 3.

PTH2R-expressing neurons in preoptic and hypothalamic regions of the mouse brain demonstrated by X-gal histochemistry in PTH2R knockin mice. **A:** $PTH2R^+$ neurons in the medial preoptic nucleus. **B:** $PTH2R^+$ neurons are particularly abundant in the posteromedial part of the medial subdivision of the bed nucleus of the stria terminalis (arrows). **C:** $PTH2R^+$ neurons in the paraventricular and periventricular hypothalamic nuclei. $PTH2R^+$ neurons are also present in the reuniens thalamic nucleus. **D:** The density of $PTH2R^+$ neurons is very high in the arcuate nucleus and high in the lateral hypothalamic area, the perifornical, and dorsomedial hypothalamic nuclei. Scale bars = 300 μm.

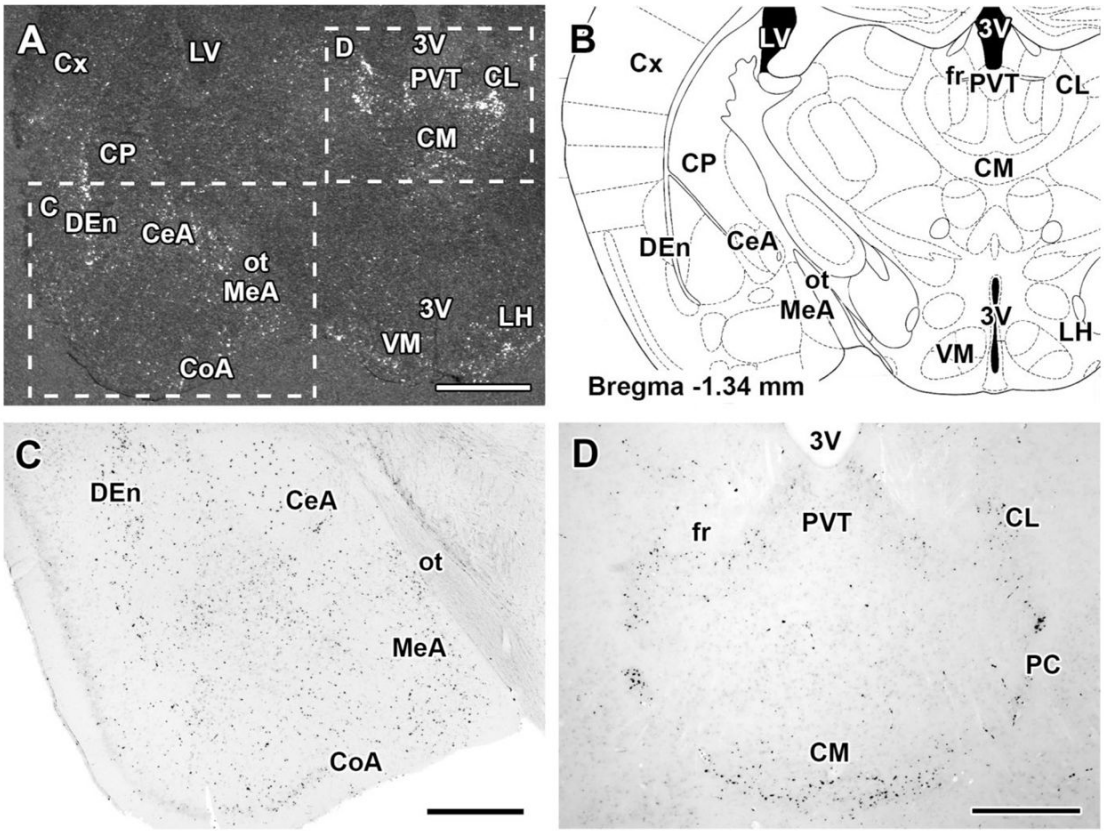

Fig. 4.

PTH2R-expressing neurons in the amygdala and dience-phalic regions of the mouse brain. **A:** Darkfield image of an in situ hybridization section demonstrates the location of PTH2R mRNA in the amygdala, the midline thalamic nuclei, and the tuberal region of the hypothalamus. **B:** Schematic diagram of the area corresponding to A. **C:** $PTH2R^+$ neurons are demonstrated by X-gal histochemistry in the amygdala of a PTH2R knockin mouse. The labeling is intense in the central, medial, and cortical amygdaloid nuclei as well as in the dorsal endopiriform nucleus. The photomicrograph corresponds to the area framed in A. **D:** X-gal histochemical labeling in the midline thalamic nuclei of a PTH2R knockin mouse. The photomicrograph corresponds to the area framed in A. $PTH2R^+$ neurons are abundant in the paraventricular, centromedian, centrolateral, and paracentral thalamic nuclei. The habenula also contains $PTH2R^+$ neurons. Scale bars = 1 mm in A; 500 μm in C; 400 μm in D.

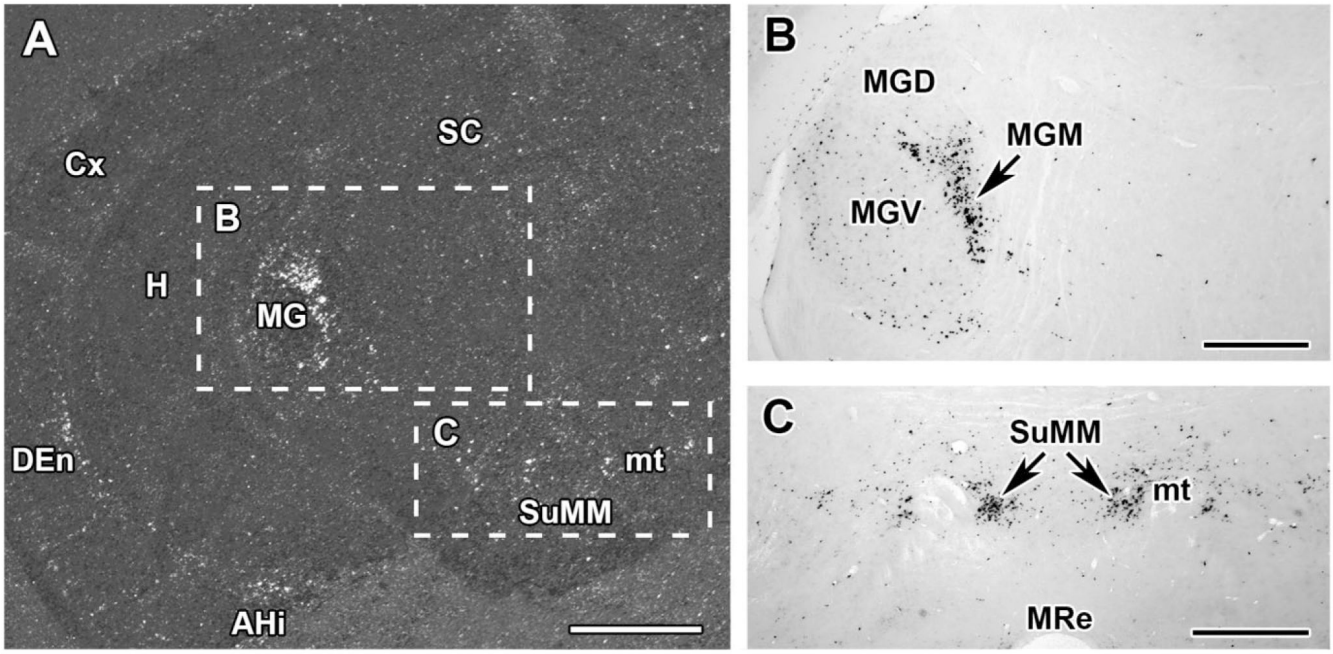

Fig. 5.

PTH2R-expressing neurons at the level of the diencephalon–midbrain junction in the mouse brain. **A:** PTH2R mRNA is shown in a darkfield photomicrograph of an in situ hybridization section. $PTH2R^+$ neurons are abundant in the medial geniculate body, the supramamillary nucleus, the dorsal endopiriform nucleus, the amygdalo-hippocampal transitional zone, and the ventral subiculum. Scattered $PTH2R^+$ neurons are also present in the cerebral cortex, the hippocampus, and the superior colliculus. **B, C:** $PTH2R^+$ neurons are demonstrated by X-gal histochemistry in a PTH2R knockin mouse in areas that correspond to the areas framed in A. In the medial geniculate body (B) the labeling is particularly intense in the medial subdivision of the medial geniculate nucleus. A relatively high density of $PTH2R^+$ neurons is also present in the ventral subdivision of the medial geniculate nucleus and in the posterior intralaminar thalamic nucleus. Within the supramamillary nucleus (C) the labeling is particularly intense in the medial subdivision. Scale bars = 1 mm in A; 400 μm in B; 500 μm in C.

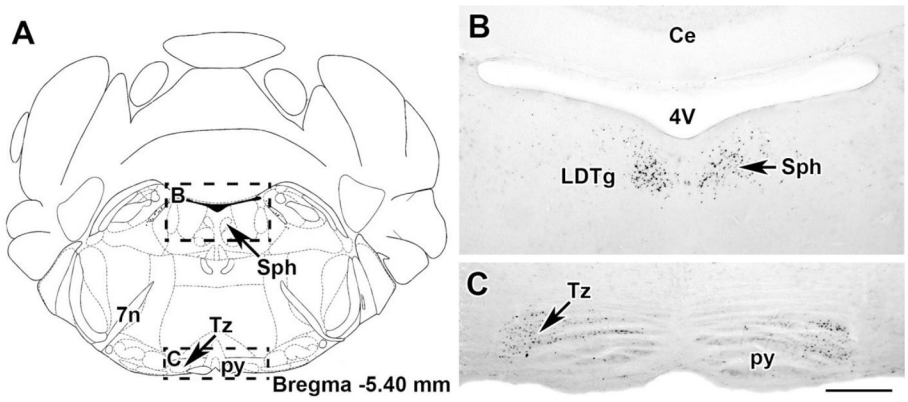

Fig. 6.

PTH2R-expressing neurons at the level of the pons in the mouse brain. **A:** A schematic diagram shows framed areas corresponding to the photomicrographs of X-gal labeled sections of PTH2R knockin mice. $PTH2R^{+}$ neurons are present in the sphenoid nucleus (**B**), and the nucleus of the trapezoid body (**C**). Scale bar = 300 μm.

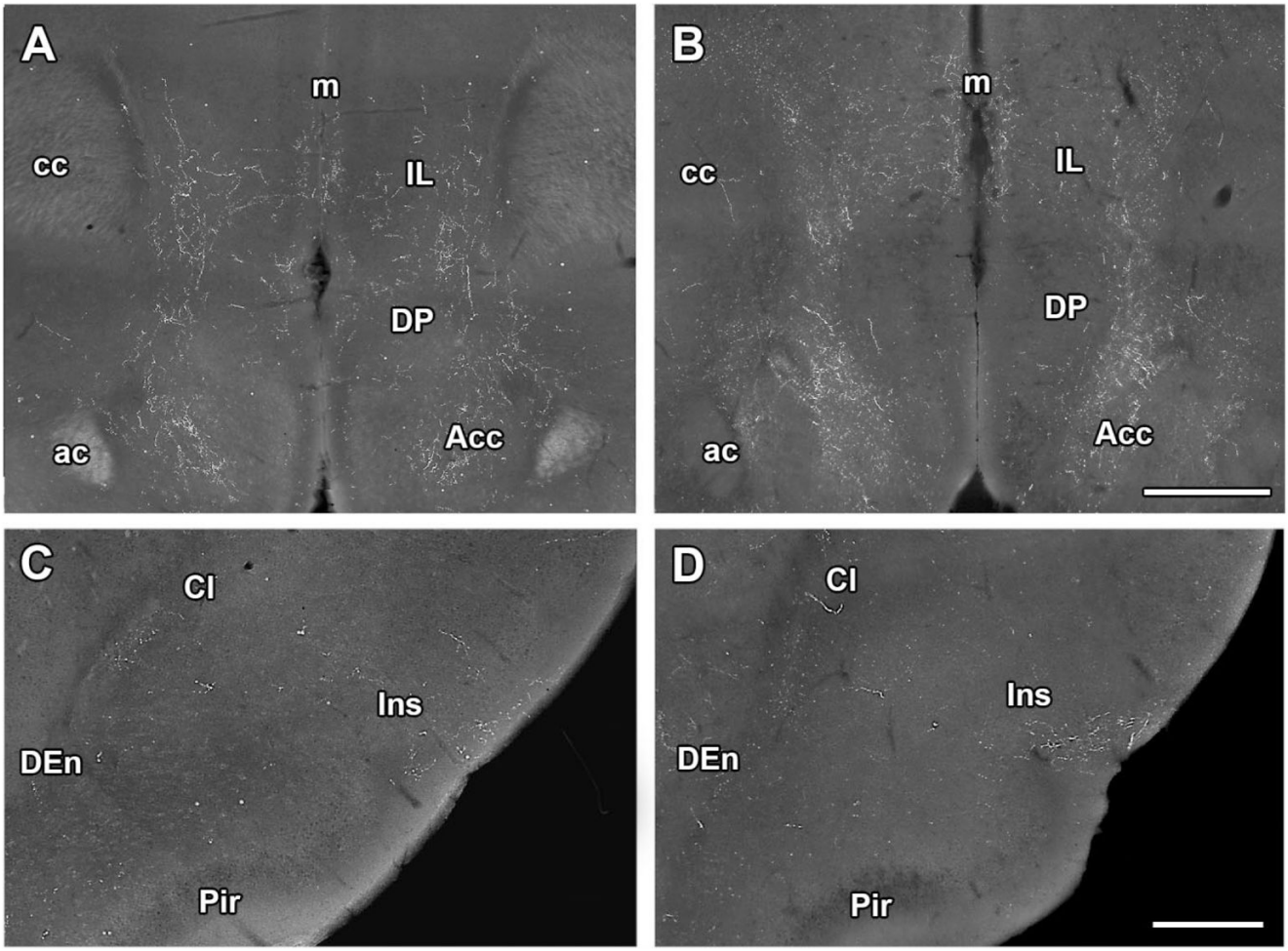

Fig. 7.

Comparison of TIP39 and PTH2R immunolabeling in the cerebral cortex. **A:** TIP39$^+$ fibers in the medial prefrontal cortex. **B:** PTH2R$^+$ fibers in the medial prefrontal cortex. Both TIP39$^+$ and PTH2R$^+$ fibers are present in the superficial as well as the deep layers of the infralimbic cortex, while other medial prefrontal cortical regions contain immunoreactive fibers only in deep layers. TIP39$^+$ and PTH2R$^+$ fibers are also abundant in the shell part of the accumbens nucleus. **C:** TIP39$^+$ fibers in the claustrum and insular cortex. **D:** PTH2R$^+$fibers in the claustrum and insular cortex. Both TIP39$^+$ and PTH2R$^+$fibers are present in the ventral part of the insular cortex but not in the piriform cortex. Medially, however, immunoreactive fibers are present in the claustrum as well as in the dorsal endopiriform nucleus. Scale bars = 500 μm in B; 300 μm in D.

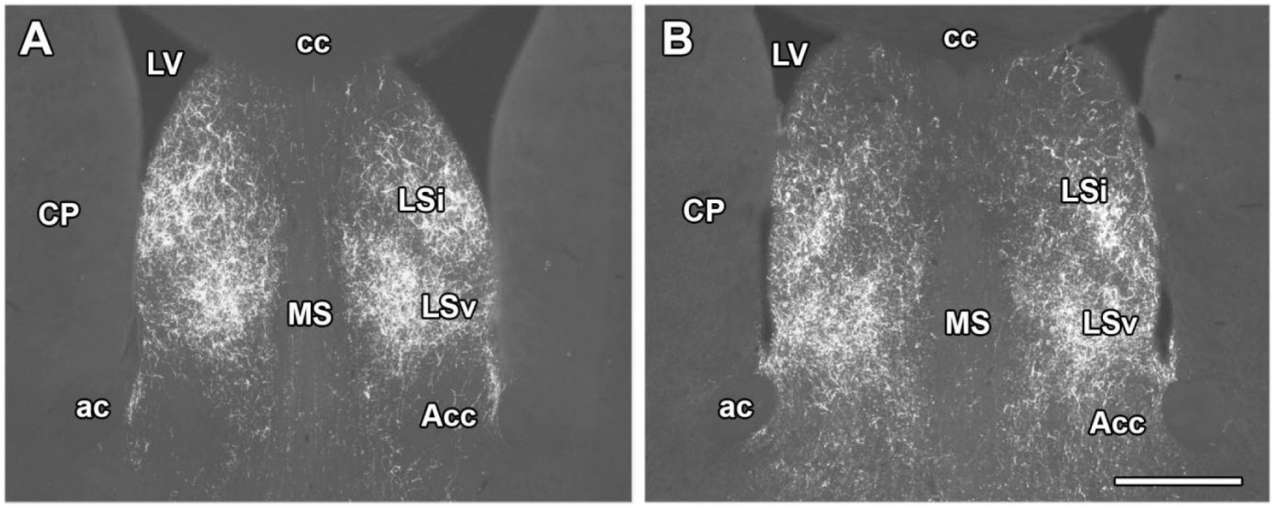

Fig. 8.

Comparison of TIP39 and PTH2R immunolabeling in the septal region. TIP39-ir (**A**) as well as PTH2R-ir (**B**) is abundant in two different layers of the intermediate and ventral subdivisions of the lateral septal nucleus. Analysis using high-magnification objectives demonstrated that the immunore-activities here are present in fibers and fiber terminals and not in cell bodies. Scale bar = 500 μm.

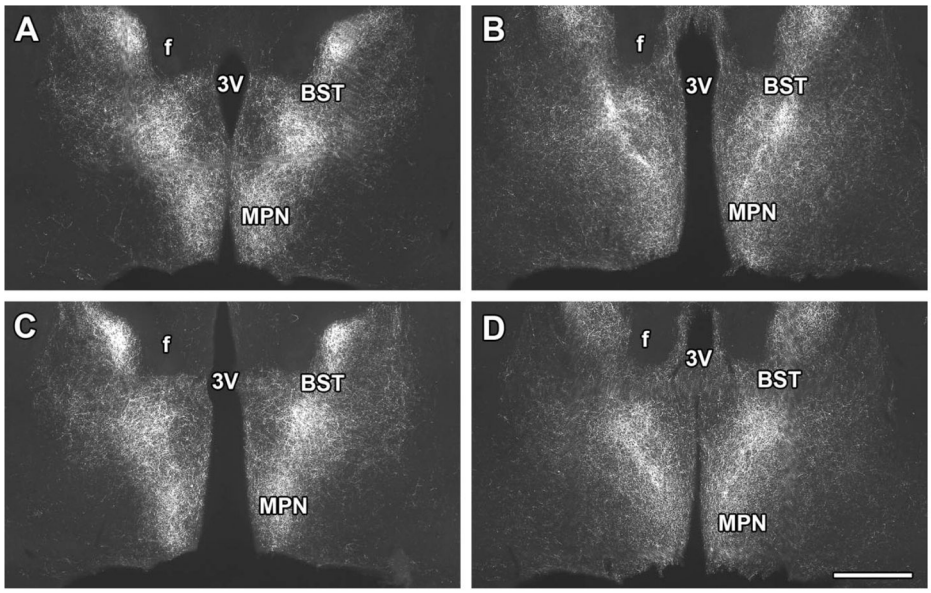

Fig. 9.

Comparison of TIP39 and PTH2R immunolabeling in the preoptic region of male and female mice. The distribution of $TIP39^+$ fibers in the male (**A**) looks exactly the same as the distribution of $TIP39^+$ fibers in the female (**B**). Similarly, the distribution of $PTH2R^+$ fibers in the male (**C**) looks exactly the same as the distribution of $PTH2R^+$ fibers in the female (**D**). In addition, the distribution of $TIP39^+$ fibers is very similar to the distribution of the PTH2R-ir. Both immunoreactivities are intense in the bed nucleus of the stria terminalis, particularly in the posteromedial part of its medial subdivision, and in the medial preoptic nucleus. Scale bar = 500 μm.

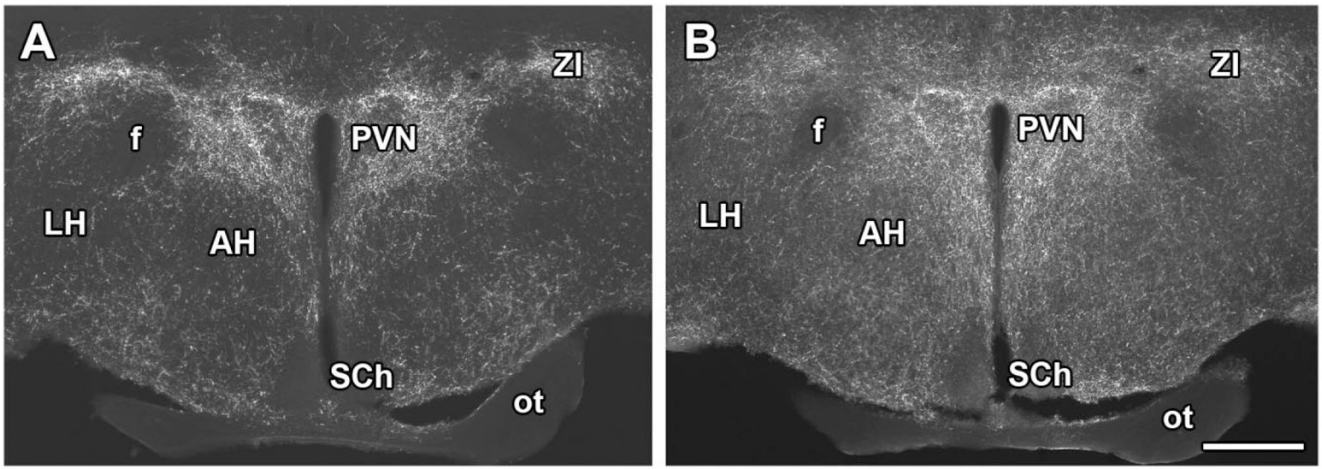

Fig. 10.

Comparison of TIP39 and PTH2R immunolabeling in the anterior hypothalamus. TIP3^{+} (**A**) as well as PTH2R^{+} fibers (**B**) are abundant in the parvicellular subdivisions of the paraventricular hypothalamic nucleus, in the periparaventricular zone, and in the zona incerta. A moderate density of immunoreactive fibers is present in the anterior hypothalamic nucleus, while the density of immunoreactive fibers is low in the magnocellular subdivisions of the paraventricular hypothalamic nucleus and in the lateral hypothalamic area. No immunoreactivity is visible in the suprachiasmatic nucleus. Scale bar = 400 μm.

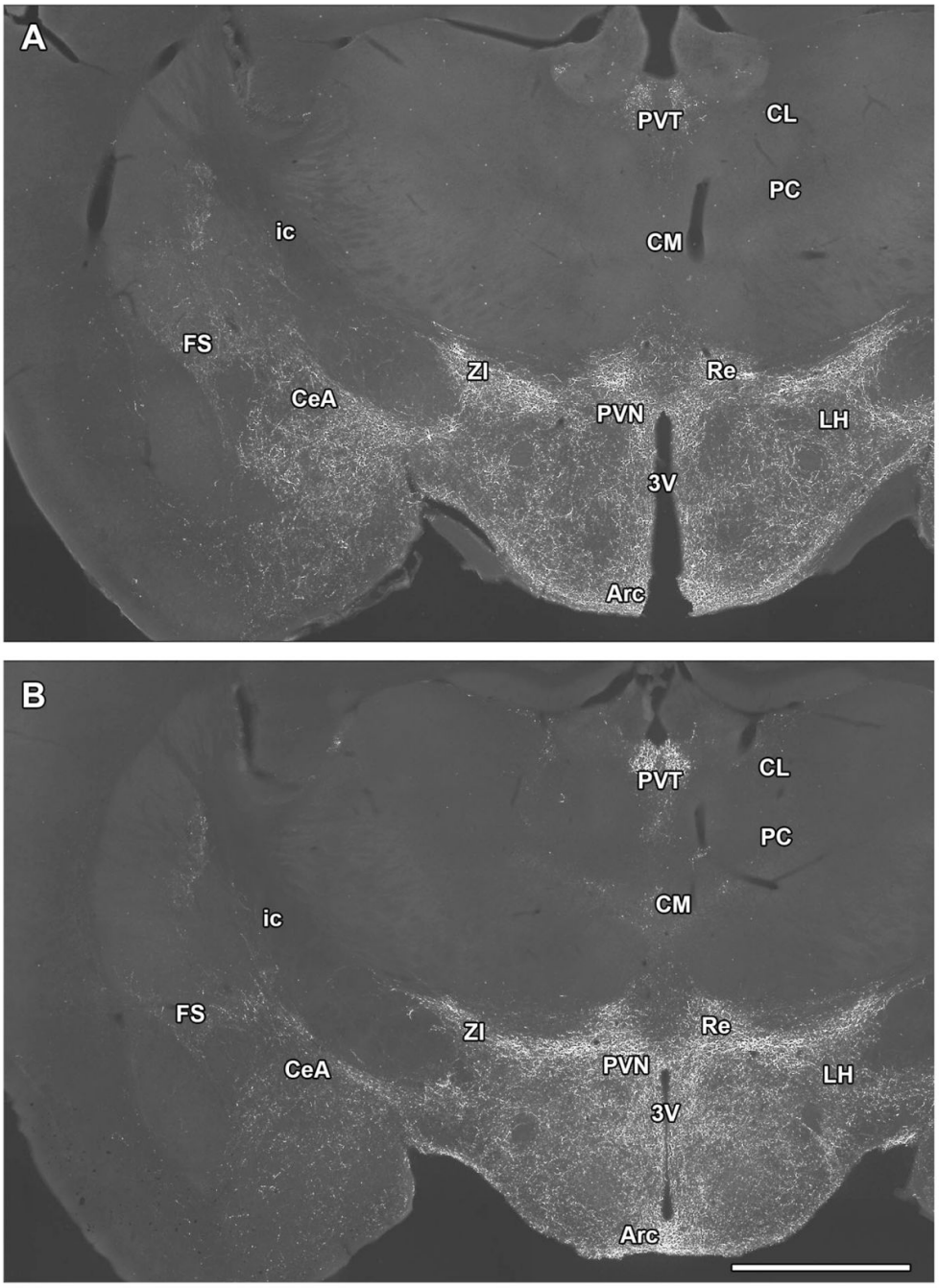

Fig. 11.

Comparison of TIP39 and PTH2R immunolabeling in the amygdala and diencephalic regions of the mouse brain. TIP39-ir (**A**) as well as PTH2R-ir (**B**) is abundant at this level of the hypothalamus including the paraventricular and periventricular hypothalamic nuclei and the arcuate nucleus. A somewhat lower density of fibers is present in the lateral hypothalamic area. Other diencephalic structures in the figure where the density of $TIP39^+$ as well as $PTH2R^+$ fibers are high include the zona incerta and the paraventricular and reuniens thalamic nuclei. A low intensity of PTH2R-ir is seen in additional midline and intralaminar thalamic nuclei including the centromedian, paracentral, and centrolateral thalamic nuclei. In the amygdaloid region $TIP39^+$ and $PTH2R^+$ fibers have the highest

density in the central amygdaloid nucleus. A lower density of fibers is also present in other amygdaloid nuclei as well as in the fundus striati. Scale bar = 1 mm.

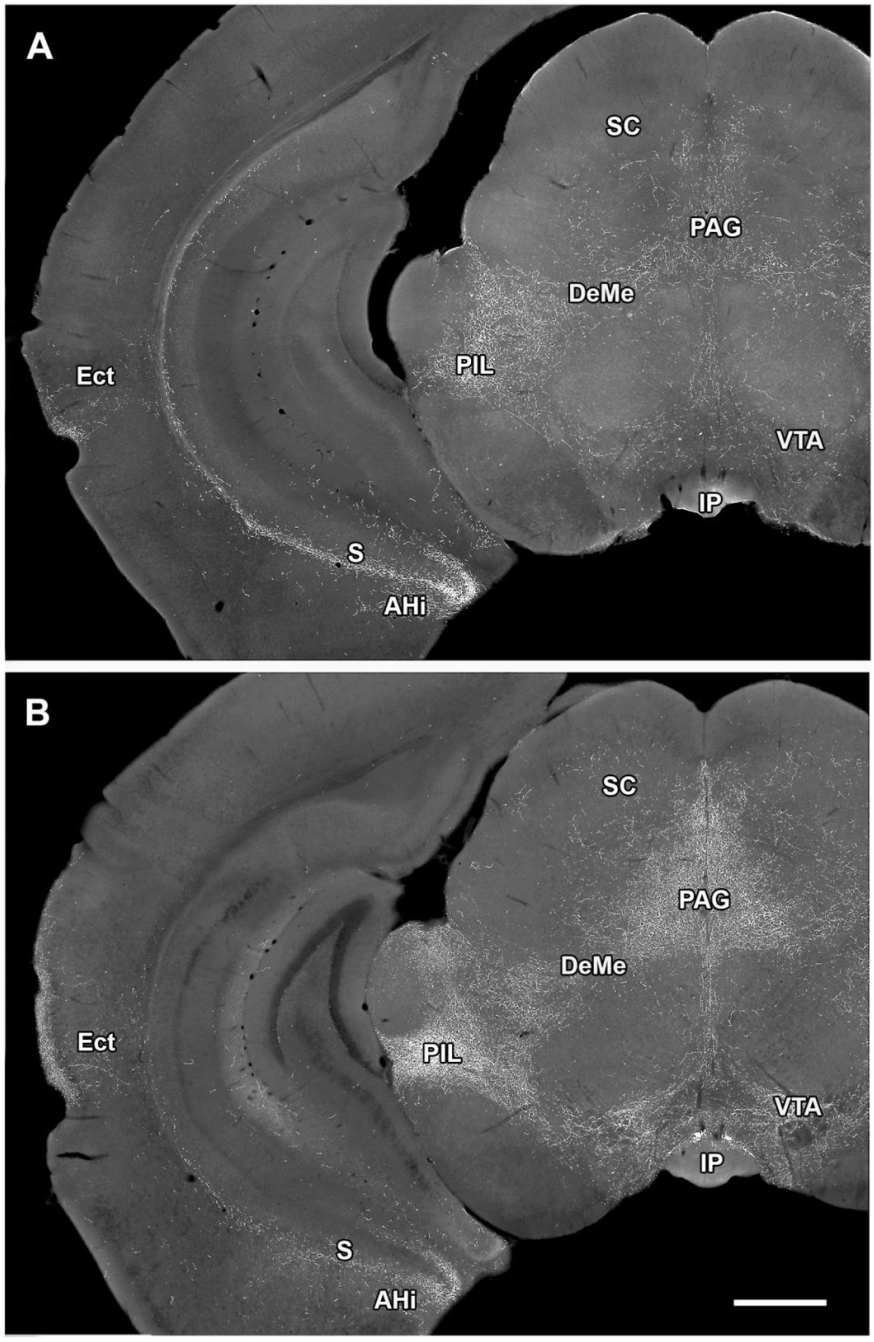

Fig. 12.

Comparison of TIP39 and PTH2R immunolabeling at the level of the rostral midbrain. TIP39-ir (**A**) as well as PTH2R-ir (**B**) is abundant at this level in the periaqueductal gray, the posterior intralaminar thalamic nuclei, the deep mesencephalic nucleus, the ventral tegmental area, the ectorhinal cortex, the amygdalo-hippocampal transitional area, and the ventral subiculum. A lower density of immunoreactive fibers is present in the deep layers of the superior colliculus. Scale bar = 1 mm.

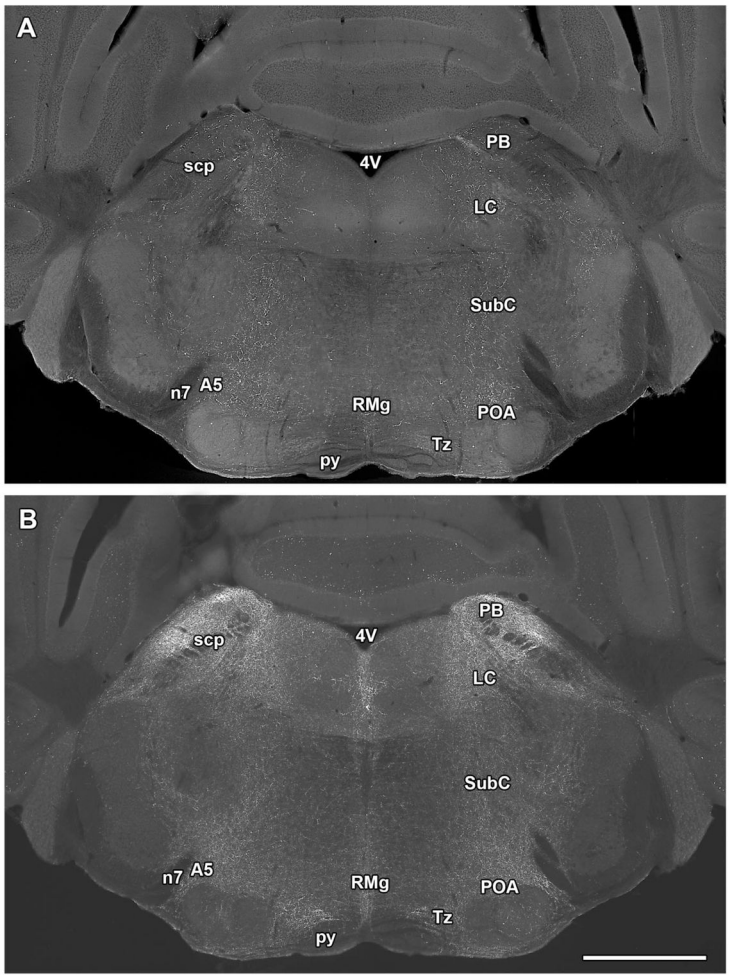

Fig. 13.

Comparison of TIP39 and PTH2R immunolabeling in the pons. The distribution of TIP39-ir (**A**) is very similar to that of PTH2R-ir (**B**). Both $TIP39^{+}$ and $PTH2R^{+}$ fibers are present in the parabrachial nuclei, the locus coeruleus, the subcoeruleus area, and the periolivary area. However, the density of fibers is considerably higher for the PTH2R, especially in the parabrachial nuclei. In addition, PTH2R immunolabeling but not TIP39 immunolabeling can be observed in the cerebellum, the tegmentum, and the nucleus of the trapezoid body. Scale bar = 1 mm.

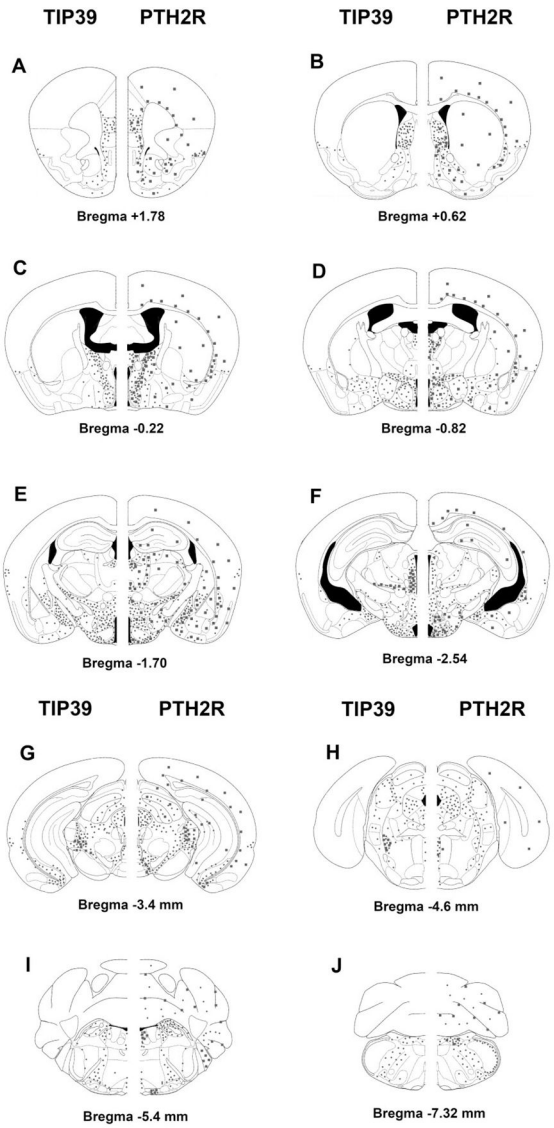

Fig. 14.

Schematic diagrams demonstrate the distribution of TIP39 and the PTH2R in the mouse brain. The diagrams are modifications from a mouse stereotaxic atlas (Franklin and Paxinos, 1997). The left side of each panel shows the location of TIP39 and the right side of each panel shows the location of the PTH2R. Dots represent fibers and fiber terminals, while squares represent cell bodies.